TECHNICAL
MEMORANDUM
NCSC TM280-80

MARCH 1980

HYDRODYNAMIC DESIGN AND ANALYSIS OF A TOWED ENVIRONMENTAL SENSOR VEHICLE

D. C. SUMMEY

NAVAL COASTAL SYSTEMS CENTER
NCSC
PANAMA CITY, FLORIDA 32407

NAVAL COASTAL SYSTEMS CENTER

PANAMA CITY, FLORIDA 32407

CAPT RAYMOND D. BENNETT, USN
Commanding Officer

GERALD G. GOULD
Technical Director

ADMINISTRATIVE INFORMATION

This work was prepared by NCSC under the direction of D. C. Summey.

Released by
Douglas E. Humphreys, Head
Hydrodynamics Division
March 1980

Under Authority of
M. J. Wynn, Head
Coastal Technology Department

UNCLASSIFIED

SECURITY CLASSIFICATION OF THIS PAGE (When Data Entered)

REPORT DOCUMENTATION PAGE

READ INSTRUCTIONS BEFORE COMPLETING FORM

1. REPORT NUMBER: NCSC-TM-280-80	2. GOVT ACCESSION NO.
3. RECIPIENT'S CATALOG NUMBER	
4. TITLE (and Subtitle): HYDRODYNAMIC DESIGN AND ANALYSIS OF A TOWED ENVIRONMENTAL SENSOR VEHICLE.	5. TYPE OF REPORT & PERIOD COVERED
	6. PERFORMING ORG. REPORT NUMBER
7. AUTHOR(s): D. C. Summey	8. CONTRACT OR GRANT NUMBER(s): 12 48
9. PERFORMING ORGANIZATION NAME AND ADDRESS: Naval Coastal Systems Center, Panama City, Florida 32407	10. PROGRAM ELEMENT, PROJECT, TASK AREA & WORK UNIT NUMBERS
11. CONTROLLING OFFICE NAME AND ADDRESS	12. REPORT DATE: Mar[redacted]80 13. NUMBER OF PAGES: 44
14. MONITORING AGENCY NAME & ADDRESS (if different from Controlling Office): 9 Technical memo	15. SECURITY CLASS. (of this report): UNCLASSIFIED 15a. DECLASSIFICATION/DOWNGRADING SCHEDULE: N/A

16. DISTRIBUTION STATEMENT (of this Report)

Approved for public release; distribution unlimited.

17. DISTRIBUTION STATEMENT (of the abstract entered in Block 20, if different from Report)

18. SUPPLEMENTARY NOTES

19. KEY WORDS (Continue on reverse side if necessary and identify by block number)

Towed vehicles
Environmental sensor
Design
Hydrodynamic stability
Performance
Stability control
Identifiers:
Hydrodynamic design
Towed environmental sensor vehicle
Environmental sensor vehicle

20. ABSTRACT (Continue on reverse side if necessary and identify by block number)

A hydrodynamic vehicle design analysis of a towed environmental sensing system was conducted. The primary thrust of the analysis was to determine the towed vehicle geometry and mass characteristics which best meet the depth-keeping and stability requirements. The effects of the tow cable, depressor, and tow ship were also examined. The design requirements, initial vehicle geometry, the effects of geometry modifications, and the final vehicle geometry are presented. Longitudinal and lateral stability are presented as a →

next page

DD FORM 1 JAN 73 1473 EDITION OF 1 NOV 65 IS OBSOLETE

S/N 0102-LF-014-6601

410650

UNCLASSIFIED

SECURITY CLASSIFICATION OF THIS PAGE (When Data Entered)

19.

Sensor vehicle
Hydrodynamic analysis techniques

20.

function of geometry. Towed vehicle response is predicted for typical seaway and ship motion forcing functions, and the system tow performance is presented as a function of speed and depth.

TABLE OF CONTENTS

LIST OF TABLES

LIST OF ILLUSTRATIONS

INTRODUCTION

The Naval Coastal Systems Center (NCSC) conducted a hydrodynamic design analysis of a towed environmental sensing system. Although the major component of the system is a sensor vehicle intended to sample seawater at a given depth at various tow speeds, the analysis also examined the effects of the tow cable, the depressor, and the tow ship. The entire system was sized and designed to satisfy a specific set of requirements. Using the semi-empirical hydrodynamic analysis methods developed at NCSC, the sensor vehicle was configured to ensure both longitudinal and lateral stability as well as to provide the required depth-keeping and vehicle frequency response. The hydrodynamics of the tow cable were analyzed to predict cable scope, trailback, and winch tension for both the definition of system performance, and the sizing and design of deck handling equipment.

This report documents the vehicle design process by presenting the design requirements, defining a base case vehicle, evaluating the effects of geometry modifications around the base case, and developing a final vehicle geometry description. Also included are predicted longitudinal and lateral vehicle response data for typical seaway and ship motion forcing functions. The system tow performance analysis discusses the cable and depressor selection, the system drag, and the basic cable performance as a function of speed and depth.

SENSOR VEHICLE DESIGN

REQUIREMENTS

The design requirements of the towed system were dictated primarily by the operational requirements of the sensor vehicle itself. The design objectives are summarized below:

(1) Operational depth, 0- 500 feet.

(2) Operational speeds, 0- 20 knots.

(3) Cylindrical section for sensor with 15-inch inside diameter, wet section including nose 44 inches, dry section 38 inches.

(4) Dry section for motion measurement package to measure pitch, roll, yaw, velocity, acceleration, and depth.

(5) An active control system will not be used.

(6) Minimize depth excursions to ± 3 feet.

(7) Minimize angle of attack excursions to ± 1 degree.

(8) Ensure that vehicle resonant period is greater than 10 seconds.

(9) Provide for the future capability to use more than one sensor vehicle for vertical profiling.

Compliance with the requirements outlined above dictated the conceptual design of the overall towed system shown in Figure 1. The medium to high speed, deep depth operation required the use of a faired cable. The size and volume requirements dictated a vehicle with an 18-inch diameter and an approximate length of 11 feet. In order to minimize sensor vehicle motions without active control, the sensor vehicle was decoupled from the main cable by using a pigtail bridle arrangement with a near neutrally buoyant sensor vehicle. The pigtailed sensor vehicle arrangement required the use of a separate depressor in order to provide the downforce necessary to achieve the desired depth; however, it also made possible, by utilizing additional cable breakouts, the use of multiple vehicles along the main cable. Once the hydrodynamic characteristics of each of the components are known, the sensor vehicle can be hydrodynamically configured to optimize the vehicle to desired performance.

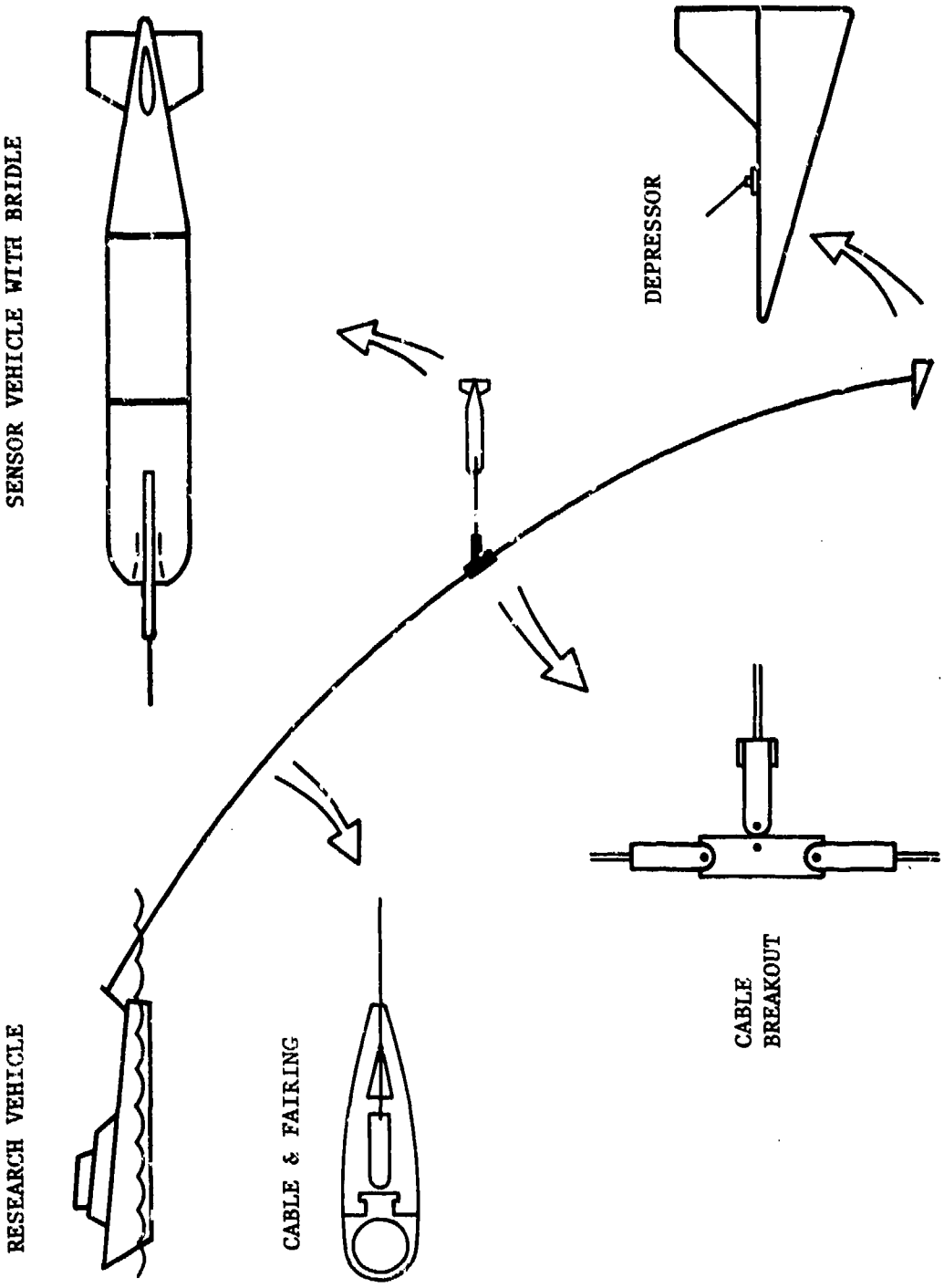

FIGURE 1. BASIC COMPONENTS FOR SENSOR VEHICLE SYSTEM

It should be noted that although the design requirements are achievable at low speeds, they become quite severe at the higher speeds. As speed increases the predictability of the vehicle motions becomes more uncertain due to the lack of a high speed data base for the semi-empirical prediction methods developed at NCSC. Therefore at speeds below 10 to 12 knots, an accurate design can be assured with a high degree of confidence; however a 20-knot design is at best risky with current dynamics prediction technology.

BASE CASE VEHICLE

The analytic process used to design an underwater vehicle at NCSC is iterative. First, a vehicle geometry is chosen which will best meet the defined requirements, and then geometry modifications are investigated which potentially may improve the vehicle dynamic response. Figure 2 shows the configuration of the base case sensor vehicle. An 18-inch diameter was chosen to meet sensor equipment housing requirements. The sensor required a flooded section of approximately 44 inches from the nose inlet. A dry hull section 38 inches long was required for the sensor electronics and motion measurement package, and the remainder of the vehicle aft of the dry section required foam to achieve neutral buoyancy. The geometric description of the base case sensor vehicle is presented in Figure 2 along with the assumed locations of the center of gravity (CG) and center of buoyancy (CB). Figure 3 depicts a computer-generated vehicle planview, while Figure 4 presents two orthographic projections and perspectives of the vehicle from different viewing angles. The mass and inertia characteristics of the vehicle are presented in Table 1.

The inlet sizes shown in Figures 3 and 4 were selected to meet internal flow requirements of the sensor at particular vehicle speeds. A tow bridle was utilized to permit the vehicle to stream freely behind the main tow cable with minimal interference with the flow inlet. The bridle/pigtail combination was chosen to decouple the vehicle from the main cable motions.

Selection of the base case vertical and horizontal tail fin size was based on preliminary analysis early in the design phase. Three fins were considered for use on the base case vehicle, and analysis indicated that while a slightly larger tail did increase the stability, the smaller tail was sufficient to provide motions within design requirements without necessitating the use of an active control system.

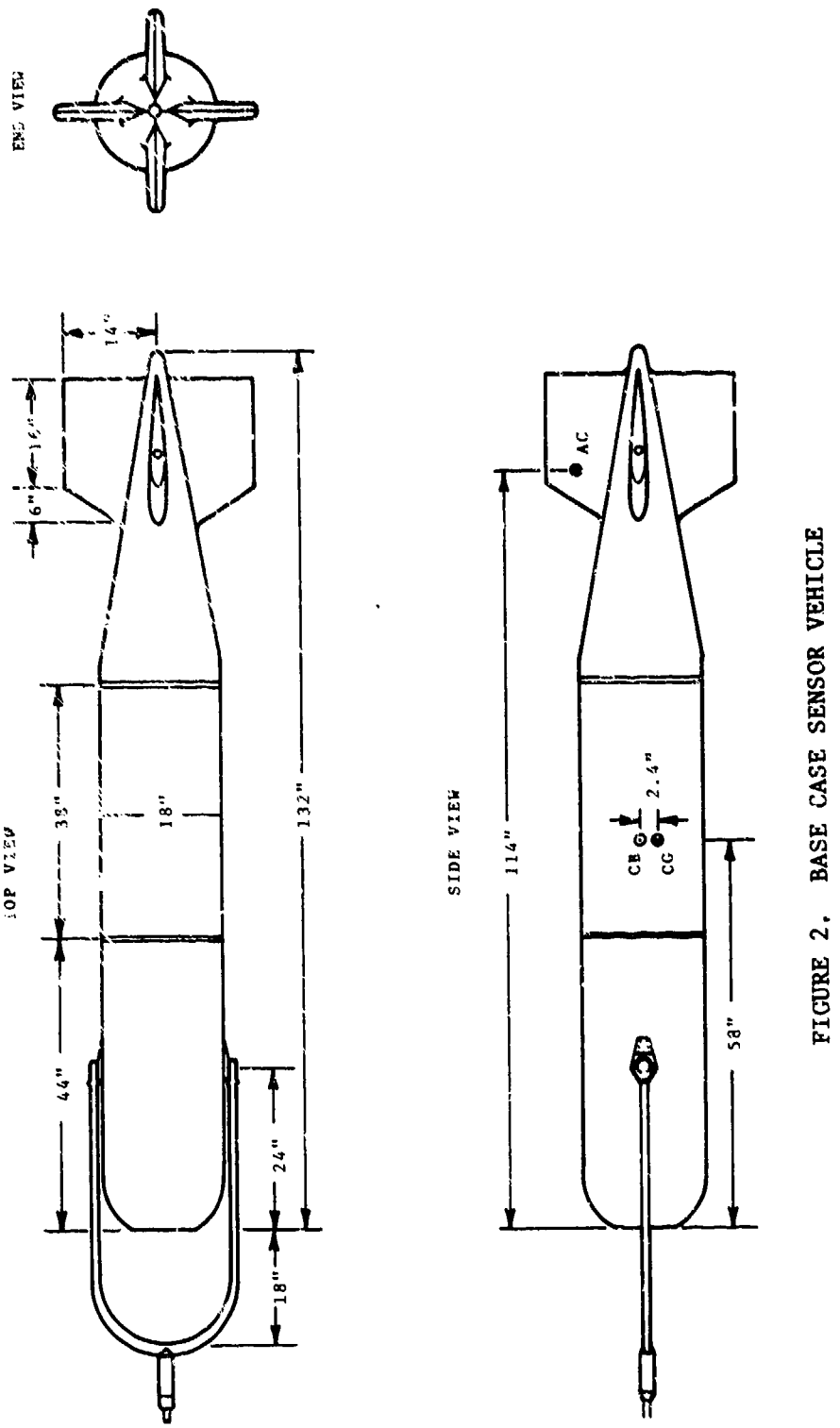

FIGURE 2. BASE CASE SENSOR VEHICLE

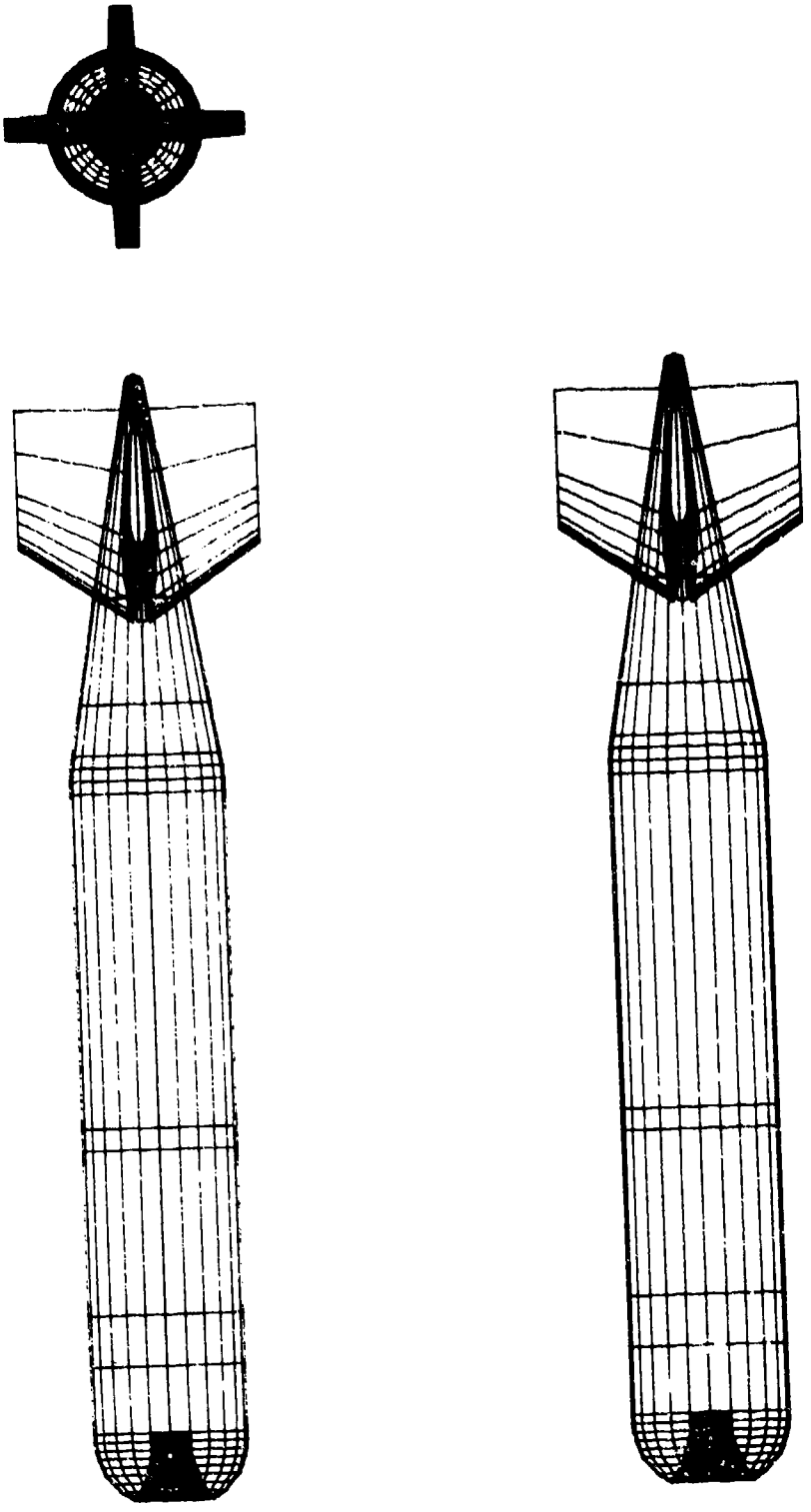

FIGURE 3. BASE CASE SENSOR VEHICLE (TOP, SIDE, AND FRONT VIEWS)

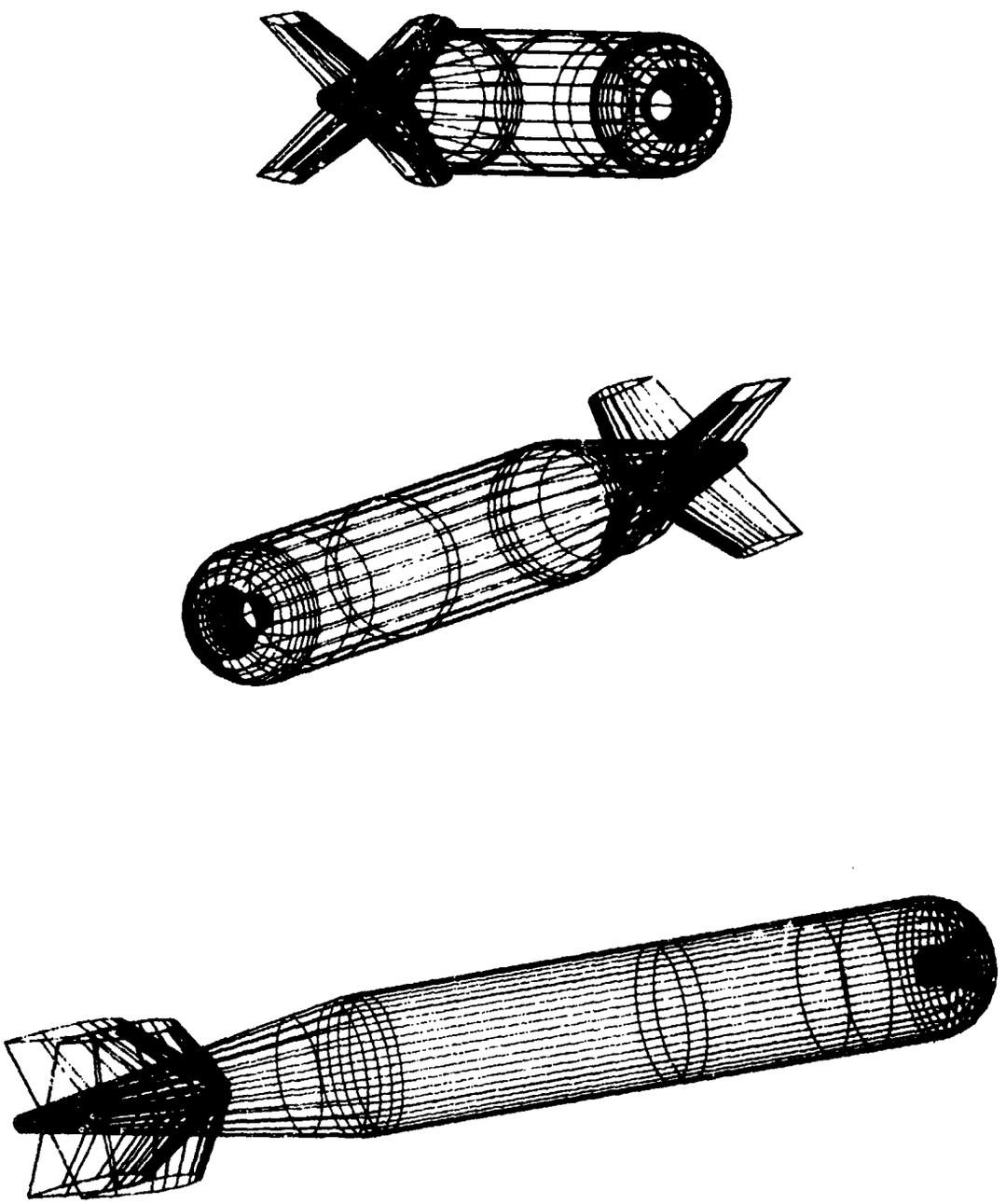

FIGURE 4. BASE CASE SENSOR VEHICLE (OBLIQUE VIEWS)

TABLE 1

MASS DISTRIBUTION DATA FOR ENVIRONMENTAL SENSOR VEHICLES

Vehicle length (ft)	11.0
Vehicle displaced weight (lb)	991.0
Body wetted area (ft^2)	42.58
Vehicle displaced volume (ft^3)	15.46
Fin planform area (ft^2)	1.48
Longitudinal location of CG (ft) (from nose)	4.83
Longitudinal location of CB (ft) (from nose)	4.83
Vertical distance CB to CG (ft) (position down)	0.2
X-axis inertia moment (slug-ft^2)	6.63
Y-axis inertia moment (slug-ft^2)	226.01
Z-axis inertia moment (slug-ft^2)	226.01

GEOMETRIC VARIATIONS

In order to determine the effectiveness of the base case design, several computer analyses were performed on the sensor vehicle with variations from the base case geometry. By analyzing the stability of these modified vehicles, a sensitivity analysis of the base case geometry was obtained in a manner similar to that presented for the GTOPS vehicle[1]. The mass and geometry characteristics of the sensor vehicle base case were defined in the previous section. The geometry variations considered here, however, also include the effects of the length of the pigtail cable and the effects of speed and buoyancy variation. So that these effects may be included, the base case pigtail length of 30 feet was selected, the vehicle was considered to be neutrally buoyant, and the base case vehicle design speed was set at 20 knots. Both

---

1 Summey, D.C., Smith, N.S., Watkinson, K.W., and Humphreys, D.E., "Hydrodynamic Stability and Control Analysis of GTOPS Vehicle," NCSC TR-323-78, May 1978.

the type and magnitude of the base case variations considered in this analysis are described in Table 2. The fin sizes and locations on the sensor afterbody are shown in Figure 5.

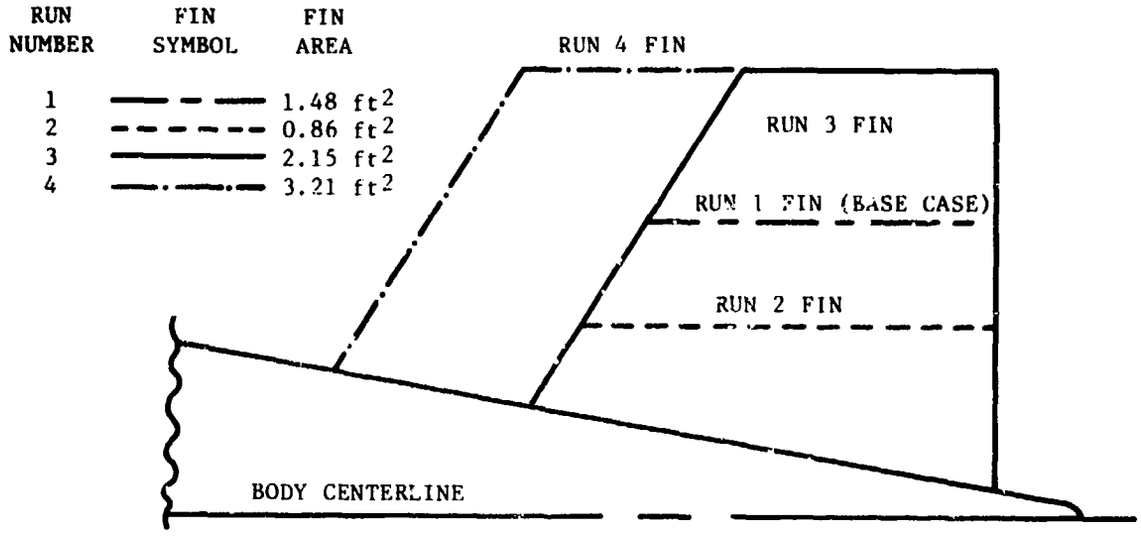

FIGURE 5. FINS CONSIDERED IN GEOMETRIC VARIATIONS

The basic stability of the various geometric configurations was determined using root locus techniques. By considering the locations of the roots of the characteristic equation of both the longitudinal and lateral transfer functions, basic system stability can be determined. A stable system must have all roots in the left-half plane (this corresponds to roots with negative real parts). Because of the near sinusoidal motion of the ship stern in response to the seaway, the forcing function for the sensor vehicle due to main cable motion is probably best described by a sine wave. With this type of frequency-dependent forcing function, a Bode plot of the vehicle response to sinusoidal excitation at various frequencies becomes a valuable analysis tool. The Bode plot not only indicates the resonant frequency and the amplitude ratio for a particular mode of motion, but it also graphically depicts the range of frequencies which will excite vehicle motions. The longitudinal and lateral characteristic roots for the geometry variations described in Table 2 are presented in Table 3. Resonant frequency and amplitude for a heaving tow point are presented for angle of attack, pitch angle, and depth change for each geometry variation in Table 4. The stability of the base case will now be considered along with a discussion of the effects of geometric variations.

TABLE 2

VEHICLE BASE CASE VARIATIONS FOR ANALYSIS

Run Number	Geometry Variation	Magnitude
1	Base Case	
2 3 4	Fin Variations (base case area = 1.48 ft^2) - See Figure 5	0.86 ft^2 2.15 ft^2 3.21 ft^2
5 6 7	Speed Variation (base case = 20 knots	15 knots 10 knots 5 knots
8 9	Pigtail length @ 20 knots (base case = 30 feet)	10 feet 50 feet
10 11	Pigtail length @ 5 knots (base case =30 feet)	10 feet 50 feet
12 13	CG-CB separation (base case CG .2 feet below)	0.1 feet 0.0 feet
14 15	Bridle length (base case 3.5 feet)	4.5 feet 2.5 feet
16 17	Net buoyarcy (base case = 0) (positive is heavy vehicle)	+ 10 pounds - 5 pounds
18 19	Longitudinal CG position (base case = 4.83 feet)	4.33 feet 5.33 feet

TABLE 3

LONGITUDINAL AND LATERAL ROOTS FOR SENSOR VEHICLE GEOMETRY VARIATIONS

Geometry Variation	Run #	Longitudinal Roots	Lateral Roots
Base Case	1	-.214 ±j 72.5 -18.2 -4.40 -.099 ±j .385	-7.57 -18.2 -4.34 -.160 ±j .526 -.528
Fin Area	2	-.184 ±j 72.5 -10.4 -3.23 -.092 ±j .332	-16.4 -2.56 ±j 1.31 -3.67 -.155 ±j .513
	3	-.241 ±j 72.4 -25.1 -3.36 -.165 ±j .532	-29.2 -4.63 -11.6 -.176 ±j .554 -.165
	4	-.274 ±j 72.4 -3.99 -23.0 -.172 ±j .534	-8.38 -25.2 -4.91 .215 ±j .668 -.114
Speed	5	-.171 ±j 72.5 -3.29 -1.37 -.087 ±j .296	-13.7 -3.25 -5.33 -.751 -.228 ±j .406
	6	-.123 ±j 72.5 -2.18 -9.08 -.079 ±j .202	-9.10 -2.08 -2.41 -1.73 -.093 ±j .282
	7	-.091 ±j .080 -1.06 -4.48 -.070 ±j 72.5	-4.54 -1.01 ±j 1.72 -1.08 -.054 ±j .15
Pigtail Length @ 20 Kts	8	-.215 ±j 72.5 -4.38 -18.2 -.110 ±j .619	-18.2 -4.27 -7.57 -.212 ± .937 -.528
	9	-.214 ±j 56.1 -4.41 -18.2 -.097 ± .30	-7.57 -18.2 -4.36 -.528 -.349 ±j .396
Pigtail Length @ 5 Kts	10	-.094 ±j .167 -1.05 -4.48 -.070 ±j 126.	-4.53 -1.01 ±j 1.72 -1.05 -.071 ±j .271
	11	-.090 ±j .032 -1.06 -4.48 -.070 ±j 56.1	-.050 ±j .113 -1.01 ±j 1.72 -1.09 -4.54
CG-CB Separation	12	-.201 ±j 72.4 -4.41 -18.2 -.092 ±j .186	-18.2 -4.35 -7.72 -.160 ±j .526 -.255
	13	-.198 ±j 72.4 -18.2 -4.41 -.085 ±j .387	-8.02 -18.2 -4.35 -.160 ±j .526 0.0
Bridle Length	14	-.215 ±j 72.5 -4.38 -18.2 -.110 ±j .619	-18.2 -4.27 -7.57 -.212 ± .937 -.528
	15	-.214 ±j 56.1 -4.41 -18.2 -.097 ± .30	-7.57 -18.2 -4.36 -.528 -.349 ±j .396
Net Buoyancy	16	-.094 ±j .167 -1.05 -4.48 -.070 ±j 126.	-4.53 -1.01 ±j 1.72 -1.05 -.071 ±j .271
	17	-.090 ±j .032 -1.06 -4.48 -.070 ±j 56.1	-.050 ±j .113 -1.01 ±j 1.72 -1.09 -4.54
Longitudinal C.G. Position	18	-.201 ±j 72.4 -4.41 -18.2 -.092 ±j .186	-18.2 -4.35 -7.72 -.160 ±j .526 -.255
	19	-.198 ±j 72.4 -18.2 -4.41 -.085 ±j .387	-8.02 -18.2 -4.35 -.160 ±j .526 0.0

TABLE 4

BODE PEAK VALUES FOR LONGITUDINAL HEAVE RESPONSE

Run #	α		θ		Z	
	Peak Value (deg/ft)	Peak Frequency (rad/sec)	Peak Value (deg/ft)	Peak Frequency (rad/sec)	Peak Value (ft/ft)	Peak Frequency (rad/sec)
1	.096	.447	1.34	.398	2.04	.355
2	.089	.355	1.07	.355	1.953	.316
3	.130	.631	1.57	.562	1.75	.501
4	.124	.631	1.53	.562	1.70	.501
5	.092	.355	1.22	.316	1.85	.282
6	.082	.251	.99	.224	1.47	.178
7	.063	.282	.518	.126	1.0	.01
8	.337	.631	3.02	.631	2.86	.631
9	.050	.355	.864	.316	1.71	.282
10	.194	.251	1.24	.20	1.17	.141
11	.038	.316	.327	.10	1.0	.01
12	.102	.447	1.45	.398	2.17	.355
13	.111	.398	1.57	.398	2.33	.398
14	.093	.355	1.28	.355	2.19	.316
15	.100	.501	1.39	.447	1.93	.398
16	.095	.447	1.34	.398	2.03	.355
17	.096	.447	1.34	.398	2.04	.355
18	.10	.447	1.37	.398	2.04	.398
19	.099	.501	1.37	.447	1.89	.398

The base case vehicle proved to be stable in both the longitudinal and lateral domain. The longitudinal characteristic equation had two pairs of oscillatory roots and a pair of aperiodic, real roots, while the lateral equation base case contained four real roots and a single oscillatory pair (See Table 3). In general, the existence of oscillatory roots means that when disturbed from equilibrium, the vehicle will overshoot while returning to equilibrium. The actual values of the real part of the root is an indication of the time required to damp to half amplitude, while the imaginary part denotes the period of the motion. The lightly damped, high frequency longitudinal oscillatory pair (imaginary part of 72.5) is the result of a simple spring mass model for the pigtail and will be discussed further in a later section. The other oscillatory pair ($-0.099 \pm j0.385$) defines the dominant longitudinal vehicle dynamics with a vehicle period of 16.3 seconds. The lateral oscillatory pair for the base case ($-0.16 \pm j0.526$) defines a lateral period of oscillation of 12 seconds.

The results of the fin size/area geometry variation can be seen by examining the roots for Runs 1 through 4 in Table 3. In the longitudinal domain the predominant effect of increasing the fin size/area (Runs 3 and 4) above the base case size is that of decreasing both the period of oscillation (base case = 16.3 seconds, well within design requirements) and the time to damp to half amplitude (base case time = 7 seconds). It should be noted that longitudinal dynamics for both large fins are almost the same. Decreasing the fin size (Run 2) increased the period of oscillation and increased the time to damp to half amplitude by about 10 percent. In the lateral mode all the fin variations affected the dominant period very little; however, they did affect the aperiodic roll root (in general the smallest real root). Increasing the fin area increased the time to damp to half amplitude in roll from 1 3 seconds to 4.2 seconds, which is less desirable. For the small fin, two of the aperiodic roots couple to create another oscillatory pair. While the large fins improve longitudinal motion slightly, they degrade lateral roll response. The smaller fin gave poor longitudinal response. The base case fin size therefore appears to be the best of those considered.

The effects of speed variation can be evaluated by examining the longitudinal and lateral root loci present in Figures 6 and 7 for depth and off-track (lateral position). Both loci indicate that several of the denominator roots are cancelled by numerator roots of almost the same value. Longitudinally, as the body is towed faster the natural period of oscillation is reduced. In passing from 5 knots to 20 knots, the period varies from 79 seconds to 16 seconds. The lateral locus exhibits the same results, in that traversing from 5 to 20 knots yields a lateral period variation of 42 to 12 seconds. Thus, the higher the speed, the more difficult it is to maintain periods greater than that specified in the design requirement.

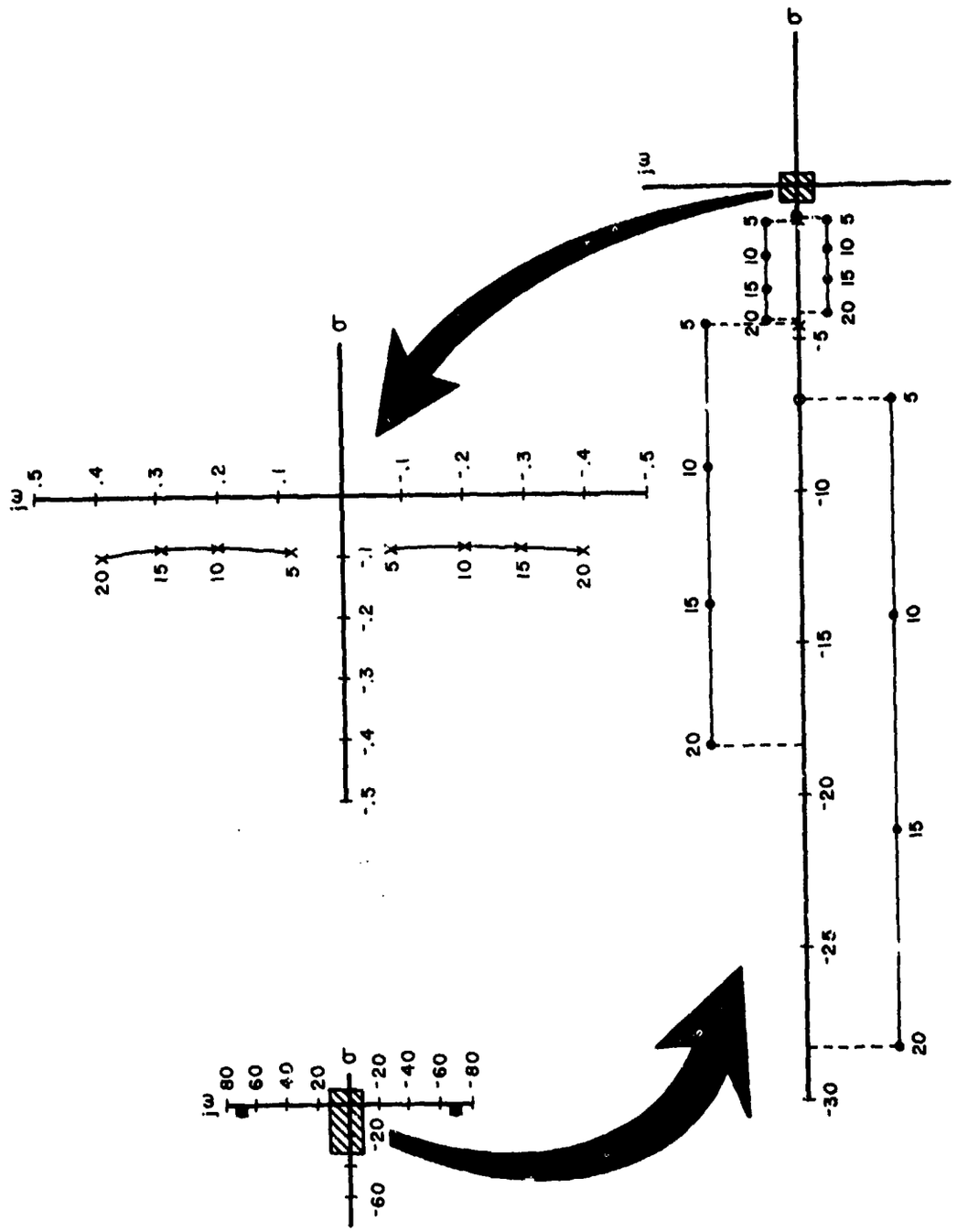

FIGURE 6. LONGITUDINAL ROOT LOCUS FOR THE TRANSFER FUNCTION OF DEPTH DUE TO A HEAVING CABLE AS A FUNCTION OF TOW SPEED

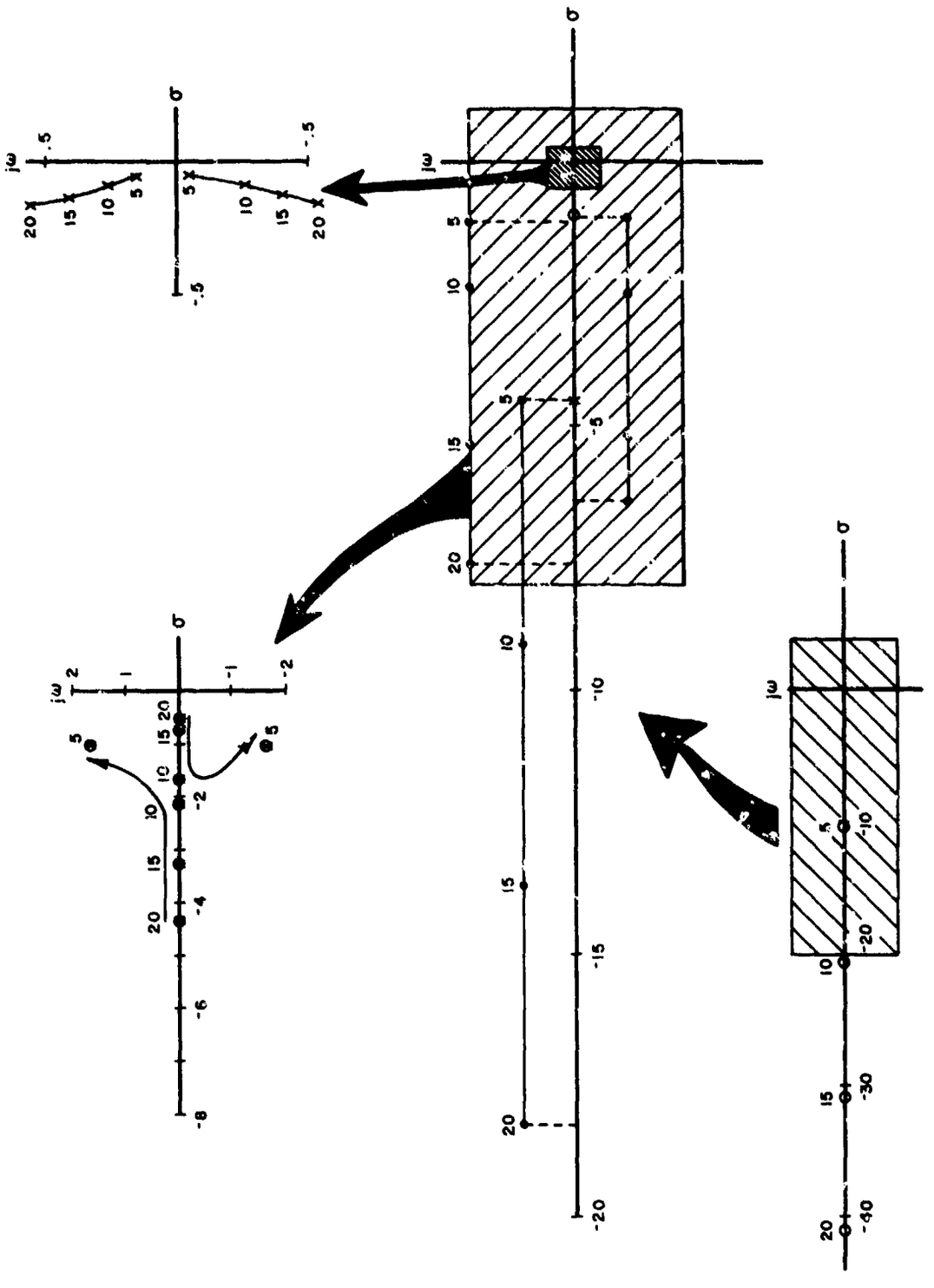

FIGURE 7. LATERAL ROOT LOCUS FOR THE TRANSFER FUNCTION OF OFF-TRACK DUE TO A SWAYING CABLE AS A FUNCTION OF TOW SPEED

The effects of varying pigtail length can best be seen by examining the Bode plot presented in Figure 8. Comparing the data, it is seen that in response to a heaving tow point motion at the cable breakout, the depth keeping capability deteriorates and the natural vehicle motion period is reduced as pigtail length is decreased. Reducing the length to 10 feet would yield motion periods outside design requirements. While increasing the length from 30 to 50 feet could improve motions slightly, the improvement is not worth the increased handling problem caused by additional cable. The effects of the same variation at a speed of 5 knots is best seen by comparing the results of Runs 10 and 11 with those of Run 7 in Table 2. For the 5-knot case, the motion amplitude is never greater than the input except in the case of the 10-foot pigtail.

Examining the roots in Table 3 shows that vertical CB-CG variation chiefly effects the roll stability. The aperiodic lateral roll root moves from -0.528 to 0.0 as the CG is moved from 0.2 feet below the CB to directly on the CB. With no separation there would be no mechanism, other than pigtail torsional stiffness (which isn't considered in this analysis), to return the vehicle to a zero roll angle if disturbed from equilibrium. Should the CG be placed above the CB, the vehicle would be unstable in roll.

The effect of the last three geometry variations — bridle length, buoyancy, and longitudinal CG position — were only minimal. The bridle variation of ±1 foot from the base only slightly modified the frequency of oscillation and time-to-damp. The buoyancy variation at 20 knots had no observable effect.* The roots presented in Table 3 for Runs 18 and 19 indicate that little change is noted in vehicle dynamics for a ±1-foot variation in longitudinal CG position.

FINAL DESIGN

Predicated on the results of the geometry variations discussed in the previous section, the base case vehicle geometry that resulted from earlier preliminary design analysis is considered optimum for meeting the design requirements of the sensor vehicle towed system. The base case vehicle itself is very stable and well within the desired design requirements. Figure 9 presents the final sensor vehicle design, showing the removable front cowling, flow outlets, the dry section, and tail cone. It should be noted that the outboard edge of each fin has been rounded to simplify fabrication. A paddle wheel vane to measure tow velocity and port and starboard acoustic pingers have been installed on the upper vertical and horizontal fins, respectively.

---

* Even though little sensitivity to buoyancy was noted, previous test experience with pigtail has suggested that both the pigtail and the vehicle must be independently neutrally buoyant to obtain acceptable vehicle motions.

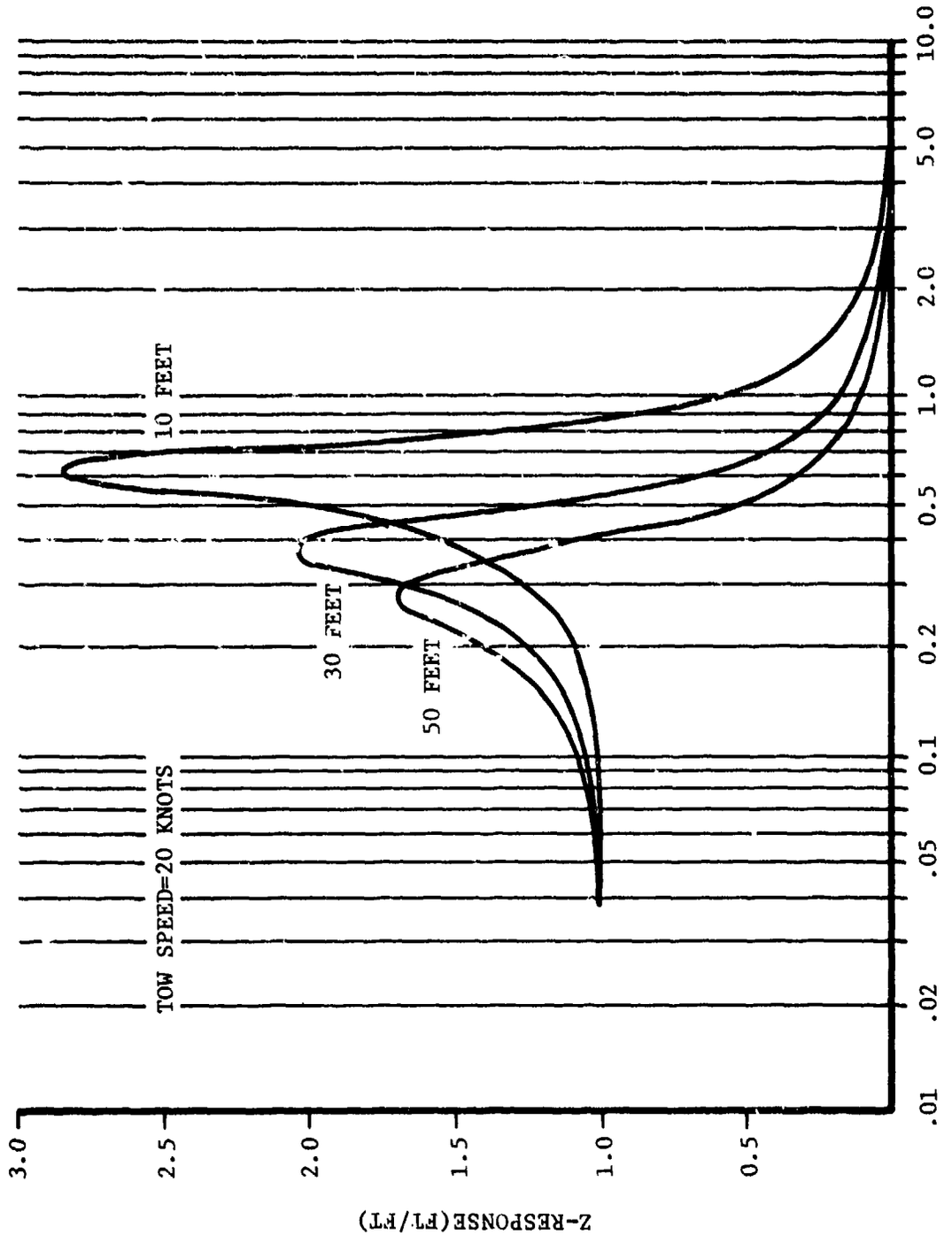

FIGURE 8. SENSOR VEHICLE RESPONSE TO A HEAVING TOW POINT FOR VARIOUS PIGTAIL LENGTHS

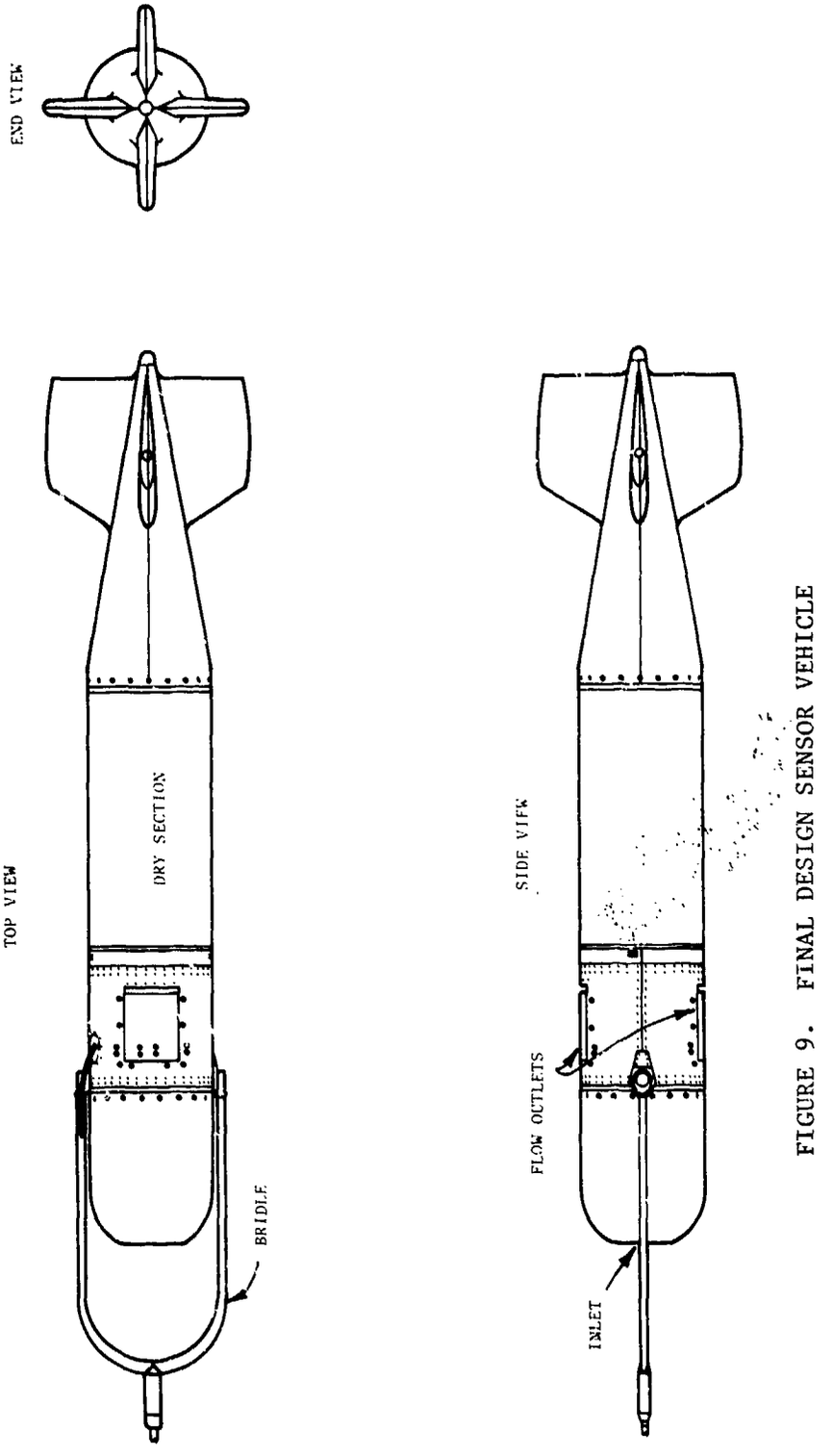

FIGURE 9. FINAL DESIGN SENSOR VEHICLE

SENSOR VEHICLE RESPONSE

FORCING FUNCTION

In order to estimate the expected sensor vehicle motions, the forcing function exciting the vehicle must be known. For the towed system considered in this study, the ship stern motion as excited by the seaway will produce an oscillatory surging, heaving type motion at the upper end of the tow cable which can potentially excite the sensor vehicle and the depressor. Once the magnitude and frequency content of the ship motion are known and it is assumed that the depressor provides no dynamic excitation forces itself at the cable breakout, the equivalent motion at the cable breakout can be approximated and can then be used to predict sensor vehicle response.

The seaway conditions off the coast of Panama City have been well documented for various seasons of the year[2,3]. Data collected in the Panama City vicinity indicate that 80 percent of the time wave heights should be less than 3 feet (Figure 10 from Reference 3). In general it was found that significant wave heights of less than 2 feet are to be expected with periods of from 2 to 6 seconds, with the majority of the energy concentrated between 4 and 6 seconds.

In order to evaluate the response of the research support platform, Response Amplitude Operator (RAO) data obtained from model tests[4] were used for a ship with a full-scale length of 160 feet. The pitch and heave RAOs were combined, neglecting phasing, to produce a worse case vertical stern motion RAO. These RAOs are presented as a function of frequency together with typical sea spectra data in Figure 11. The effects of surging motion have been neglected, since in general surge effects are small for 160-foot ships excited by sea state 2 seas. The significant (average one-third highest) vertical stern motions for each of the spectra of interest are presented in Table 5.

---

2 U.S. Navy Mine Defense Laboratory Technical Paper No. TP161, "On the Nearshore Marine Environment of the Gulf of Mexico at Panama City, Florida," by W.H. Tolbert and G.B. Austin, May 1959.

3 Naval Coastal Systems Laboratory Report 337-78, "Environmental Conditions in Coastal Waters Near Panama City, Florida," by G.G. Salsman and A.J. Ciesluk, August 1978.

4 Naval Ship Research and Development Center Report No. C-1655, "Comparative Seaworthiness Tests on Two Designs of a Patrol Gunboat, Motor," F.M. Schwartz, June 1964.

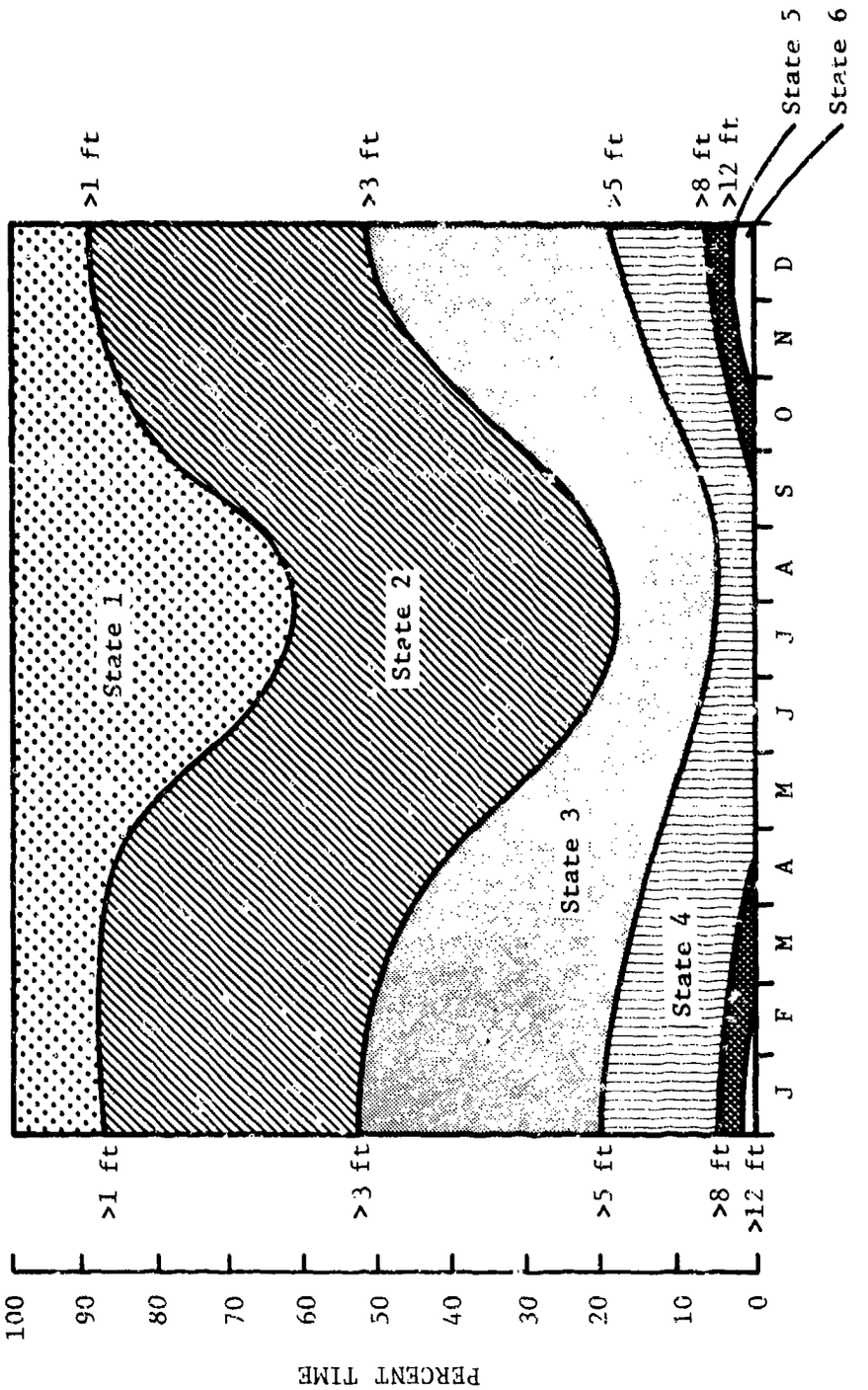

FIGURE 10. EXPECTED WAVE HEIGHTS AT PANAMA CITY
(From Reference 3)

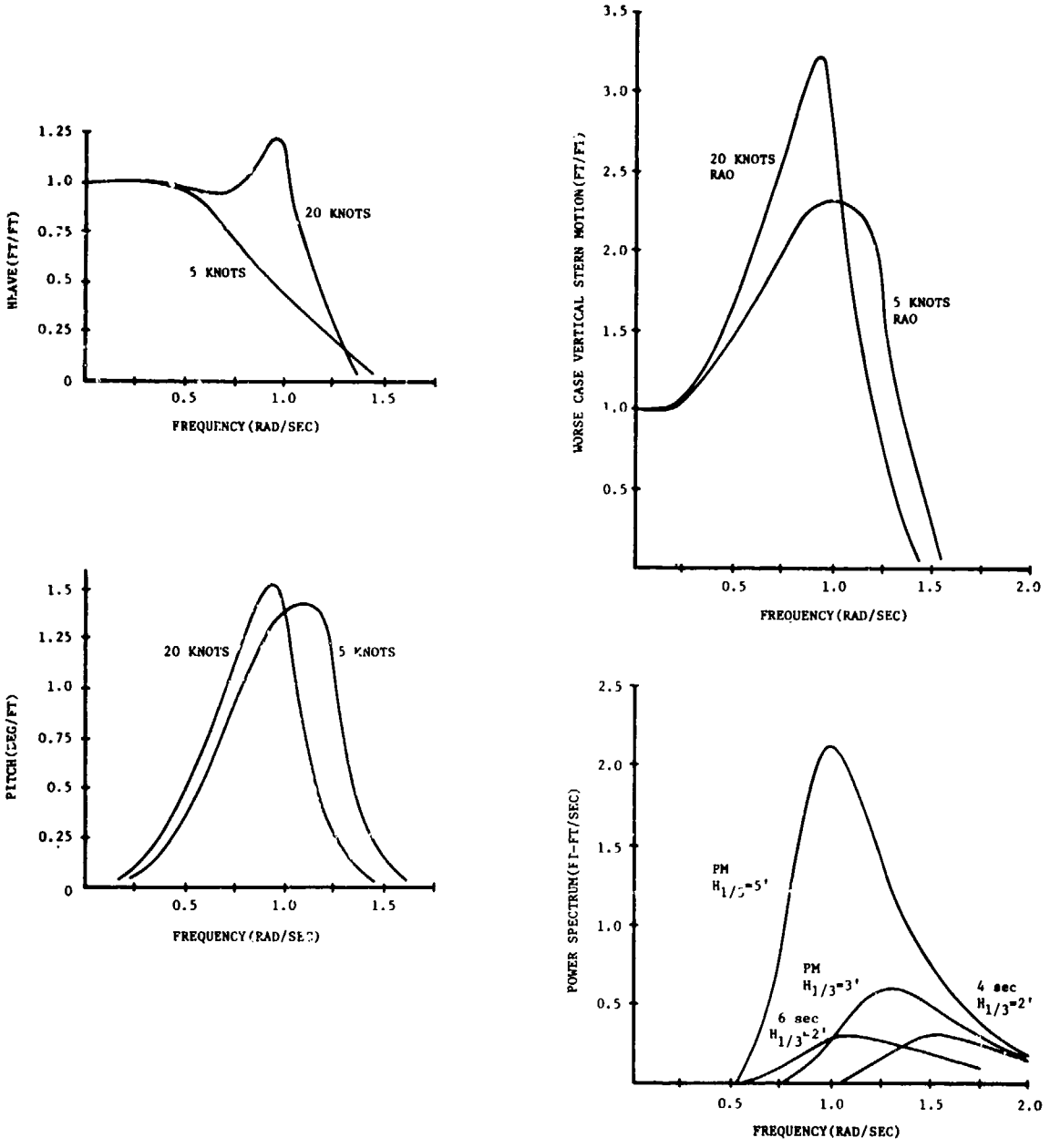

FIGURE 11. TYPICAL SHIP MOTION AND SEA SPECTRA FORCING FUNCTION DATA

TABLE 5

VERTICAL STERN MOTION FOR SEVERAL SEA SPECTRA AT TWO SPEEDS

STERN MOTION AMPLITUDES IN FEET				
WAVE SPECTRA / SPEEDS	4-SECOND	6-SECOND	PIERSON-MOSKOWITZ	PIERSON-MOSKOWITZ
	$H_{1/3}$=2 feet	$H_{1/3}$=2 feet	$H_{1/3}$=3 feet	$H_{1/3}$=5 feet
20 knots	0.32	1.84	1.61	5.04
5 knots	0.51	1.83	1.70	4.28

Examination of Table 5 indicates that if 4-second/2-foot waves are encountered, then the maximum stern motion should not exceed ±0.5 feet. If 6-second/2-foot waves exist, the stern motions should not exceed ±1.84 feet. It should be noted that for sea state 3 ($H_{1/3}$=5.0 feet) and sea state 2 ($H_{1/3}$=3.0 feet) seas, the stern motions do not exceed ±5.0 and ±1.7 feet, respectively. Based on the anticipated site conditions off Panama City, it is resaonable to assume that stern motions as large as ±1.84 feet may be encountered. In the absence of a dynamic cable analysis to predict how the motions are transmitted down the cable, it will be assumed that a ±1-foot disturbance will be damped to ±0.6 feet at the cable breakout for a tow depth of 500 feet. The exciting motions at the front of the sensor vehicle pigtail may be as large as ±1.1 feet. It should be noted that the amplitude of the forcing function is heavily dependent on the frequency at which the seaway energy is concentrated. Should the wave have longer than a 6.0 second period, the motion amplitude may be considerably increased above the ±1.1 feet. Attention will now be directed to the response of the sensor vehicle to forcing motion applied at the front of the vehicle pigtail.

VEHICLE MOTIONS

The longitudinal and lateral motion response for the sensor vehicle will now be presented in the forms of both Bode and vehicle time history plots. The hydrodynamic coefficients of the final vehicle design are presented in Table 6. The numerator and denominator roots and gains for the longitudinal angle of attack, pitch angle and depth change transfer functions for a pure heaving tow point are contained in

TABLE 6

NON-DIMENSIONAL LONGITUDINAL AND LATERAL HYDRODYNAMIC COEFFICIENTS FOR THE ENVIORNMENTAL SENSOR VEHICLE

$X'_{uu} = -0.3101 \times 10^{-2}$	$Z'_{uu} = 0.0$	$M'_{uu} = 0.0$
$X'_{w} = 0.0$	$Z'_{w} = -0.9181 \times 10^{-1}$	$M'_{w} = -0.1882 \times 10^{-1}$
$X'_{q} = -0.4188 \times 10^{-3}$	$Z'_{q} = -0.4188 \times 10^{-1}$	$M'_{q} = -0.1826 \times 10^{-1}$
$X'_{\theta} = 0.0$	$Z'_{\theta} = 0.1673 \times 10^{-2}$	$M'_{\theta} = -0.5617 \times 10^{-3}$
$X'_{\dot{u}} = -0.7768 \times 10^{-3}$	$Z'_{\dot{u}} = 0.0$	$M'_{\dot{u}} = 0.0$
$X'_{\dot{w}} = 0.0$	$Z'_{\dot{w}} = -0.2507 \times 10^{-1}$	$M'_{\dot{w}} = -0.1388 \times 10^{-2}$
$X'_{\dot{q}} = 0.0$	$Z'_{\dot{q}} = -0.1388 \times 10^{-2}$	$M'_{\dot{q}} = -0.1746 \times 10^{-2}$
$X'_{x} = -0.5066 \times 10^{-3}$	$Z'_{x} = 0.0$	$M'_{x} = 0.0$
$X'_{z} = 0.0$	$Z'_{z} = -0.5066 \times 10^{-3}$	$M'_{z} = 0.1303 \times 10^{-3}$

$Y'_{v} = -0.9181 \times 10^{-1}$	$K'_{v} = 0.0$	$N'_{v} = 0.1882 \times 10^{-1}$
$Y'_{p} = 0.0$	$K'_{p} = -0.8162 \times 10^{-3}$	$N'_{p} = 0.0$
$Y'_{r} = 0.4188 \times 10^{-1}$	$K'_{r} = 0.0$	$N'_{r} = -0.1826 \times 10^{-1}$
$Y'_{\phi} = 0.1280 \times 10^{-12}$	$K'_{\phi} = -0.1313 \times 10^{-3}$	$N'_{\phi} = 0.7053 \times 10^{-12}$
$Y'_{\psi} = -0.1868 \times 10^{-2}$	$K'_{\psi} = 0.4229 \times 10^{-12}$	$N'_{\psi} = -0.1075 \times 10^{-2}$
$Y'_{\dot{v}} = -0.2507 \times 10^{-1}$	$K'_{\dot{v}} = 0.0$	$N'_{\dot{v}} = 0.1388 \times 10^{-2}$
$Y'_{\dot{p}} = 0.0$	$K'_{\dot{p}} = -0.2711 \times 10^{-3}$	$N'_{\dot{p}} = 0.0$
$Y'_{\dot{r}} = 0.1388 \times 10^{-2}$	$K'_{\dot{r}} = 0.0$	$N'_{\dot{r}} = -0.1746 \times 10^{-2}$
$Y'_{y} = -0.5657 \times 10^{-3}$	$K'_{y} = 0.1280 \times 10^{-12}$	$N'_{y} = -0.3255 \times 10^{-3}$

Table 7. Similar lateral data are presented in Table 8 for the sideslip, heading, and roll angles, and lateral position for a pure swaying tow point. The numerator and denominator roots together with the corresponding gain values completely specify the transfer function for the dependent variables of interest; it should be remembered, however, that these transfer functions are good only for the 20-knot speed case.

The ship stern motion providing the forcing function at the cable breakout can best be modeled by a unit amplitude sinusoidal of a given frequency forcing the sensor vehicle pigtail attachment point to the main cable. The vehicle longitudinal response to all sinusoidal frequencies are presented in the Bode plots of Figure 12 for speeds of 5, 10, 15, and 20 knots. The frequency (ω) in radians per second can be specified in the form of a period, using the relation $P = 2\pi/\omega$. By examining the Z response for 20 knots, it is seen that if an exciting frequency of 0.38 (a period of 16.5 seconds) radians per second is used to force the body, depth change will be twice the amplitude of the forcing function, and similarly a 6.0 second sine wave ($\omega = 1.05$) would yield a depth change of 0.2 times the forcing amplitude. At frequencies greater than the peak (resonant) value, the response quickly falls off at a rate of approximately 10 decibels per octave. As the speed is reduced below 20 knots both the peak value of the resonant frequency and the peak frequency are reduced. The 5-knot depth response is overdamped in that the response is always less than the forcing function amplitude. Similar behavior is noted for the pitch and angle of attack responses; as speed is decreased both the peak value and the resonant frequency are reduced. The pitch angle and angle of attack for 20 knots at the resonant frequency are 1.34 and 0.1 degrees, respectively.

If the peak value of the response curve was used to predict vehicle motion, then for a 20-knot tow with a ±1.1 foot excitation the depth of the sensor vehicle would be ±2.2 feet. However, if the excitation frequency of 1.05 (6-second wave) is used, then the depth variation of ±0.2 feet is achieved; 4-second waves will yield even smaller responses. If the frequency content of the stern motions is translated directly down the cable, and if 2-foot/6-second seas are encountered, then the longitudinal vehicle response of the vehicle will involve a depth change of $\leq$0.2 feet, pitch angles of $\leq$0.33 degrees and angles of attack of $\leq$0.06 degrees. A dynamic cable model is necessary to determine the precise magnitude and frequency content of the disturbance transmitted down the cable. In the absence of such a model, an upper bound on motions for the 2-foot seas can be approximated by using the peak value of the 20-knot vehicle response curves. The upper bound for longitudinal motions are:

TABLE 7

LONGITUDINAL DENOMINATOR AND NUMERATOR ROOTS WITH TRANSFER FUNCTION GAINS FOR SINUSOIDAL HEAVE FORCING FUNCTION

	GAIN	ROOTS			
Characteristic Equation		-0.0214 ±j 72.44	-18.23	-4.402	-0.0993 ±j 0.385
$N^{\alpha}_{\Delta z}$	0.189	-0.215 ±j 72.43	-20.12	-0.018	0.0
$N^{\theta}_{\Delta z}$	-2.286	-0.198 ±j 72.36	-9.42	0.0	
$N^{z}_{\Delta z}$	0.111	-0.225 ±j 72.43	-28.16	-4.053	

TABLE 8

LATERAL DENOMINATOR AND NUMERATOR ROOTS WITH TRANSFER FUNCTION GAINS FOR SINUSOIDAL SWAY FORCING FUNCTION

	GAIN	ROOTS				
Characteristic Equation		-18.23	-7.571	-0.528	-4.344	-0.160 ±j 0.526
$N^{\phi}_{\Delta y}$	0.24	-22.87	-7.354	-0.529	0.0	0.0
$N^{\psi}_{\Delta y}$	5.38	-8.436	-6.762	-0.529	0.0	
$N^{\theta}_{\Delta y}$	1.0	-40.97	-4.164	0.0	0.0	
$N^{y}_{\Delta y}$	0.142	-40.97	-7.488	-0.529	-4.164	

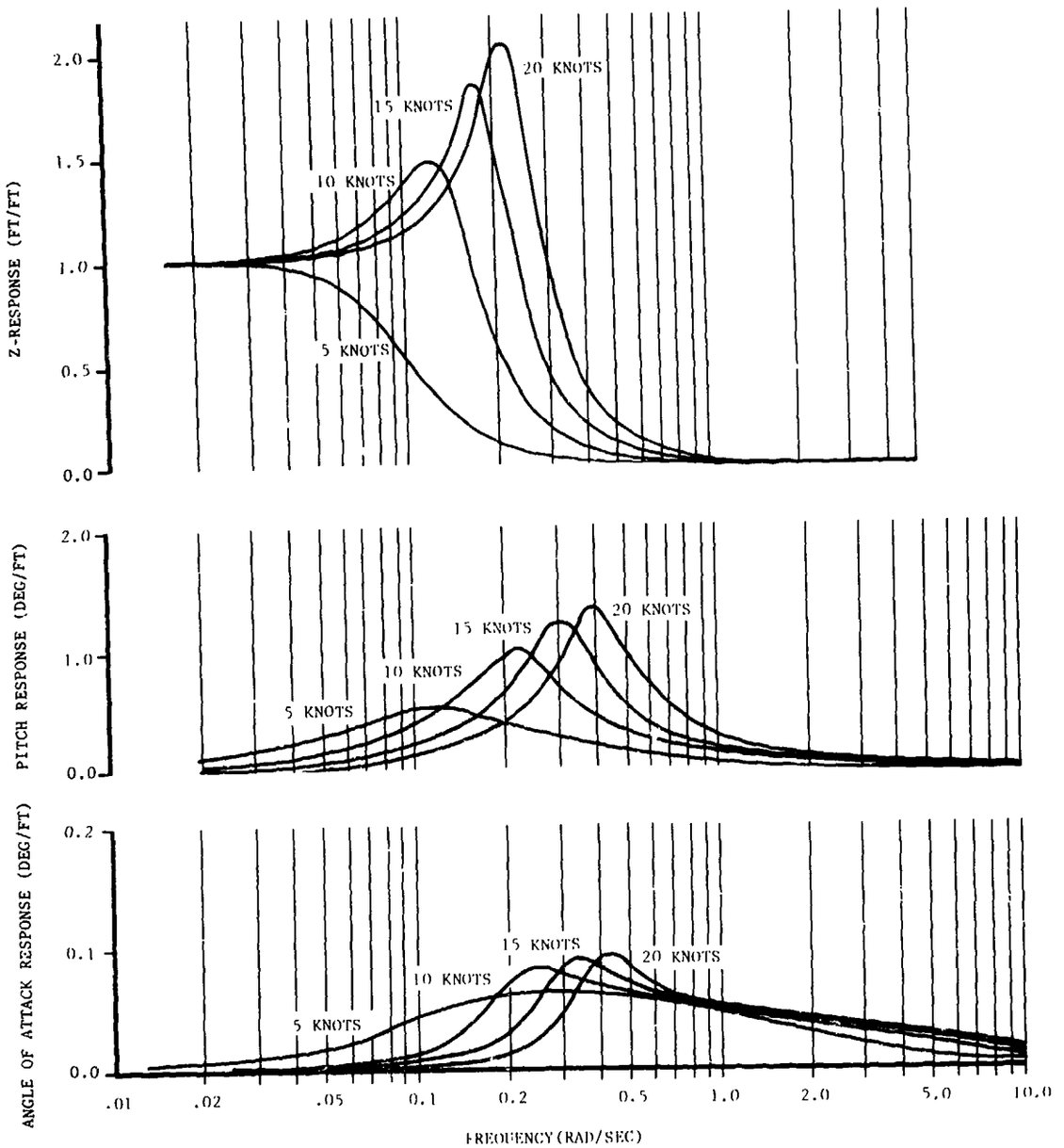

FIGURE 12. DEPTH, PITCH, AND ANGLE OF ATTACK RESPONSES OF SENSOR VEHICLE TO A HEAVING TOW POINT AT VARIOUS SPEEDS

maximum vehicle depth variation = ±2.2 feet,

maximum vehicle pitch angle variation = ±1.48 degrees,

maximum vehicle angle of attack variation = ±0.11 degrees.

The response curves can be utilized in a similar manner to predict the response at different speeds and for forcing functions with various frequency content.

The longitudinal transfer function time history plots shown in Figure 13 validate the fact that if the vehicle is excited by a ±1.0 amplitude sine wave at a frequency of 0.3858 radians per second (period = 16.3 seconds), then the vehicle response is sinusoidal with the magnitudes reflected by the Bode plots. Also presented in this figure is the response to an 8-second pulse Z-position of the pigtail/cable attachment point applied at t = 0.0 second and taken out at t = 8.0 seconds. The response to the pulse dies out completely after 40 seconds, and the period of oscillation is approximately 16 seconds. It should also be noted that the high frequency root due to cable stretch did not appear in the vehicle dynamics even for the pulse response. As can be seen in the longitudinal transfer function roots presented in Table 7, the numerators of each transfer function contain roots which almost exactly cancel the corresponding denominator roots. Thus, if the exciting motion is predominantly heave at the cable breakout, which it is, then the high frequency response will not even appear for a pulse forcing function. The frequency content of the ship motion is so low that 72 radians per second will never be approached from ship motion excitation. Therefore, even though the resonant frequency exists, it should never be excited under normal tow conditions.

The lateral frequency response plots presented in Figure 14 correspond to a pure sway motion. These plots have been included for the sake of completeness; however sway exciting forces are not anticipated. The mechanisms for generating sway at the pigtail attachment point are depressor motion, ship motion, turning maneuvers, and dynamic cable motion. The depressor should induce little lateral oscillation, since any small ship lateral motion should damp out by the time tow depth is reached and any dynamic oscillations arising from the high-speed tow of the main cable are as yet unknown. It should be noted, however, that cable fairing had been utilized to eliminate cable kiting and strumming. Although moderate and high-speed turning maneuvers by the ship will induce lateral motions on the vehicle, it was beyond the scope of this analysis to predict the response to such turning maneuvers. Should lateral forcing functions be identified, the transfer functions presented in Table 8 and the frequency response plots will be useful in determining lateral vehicle response.

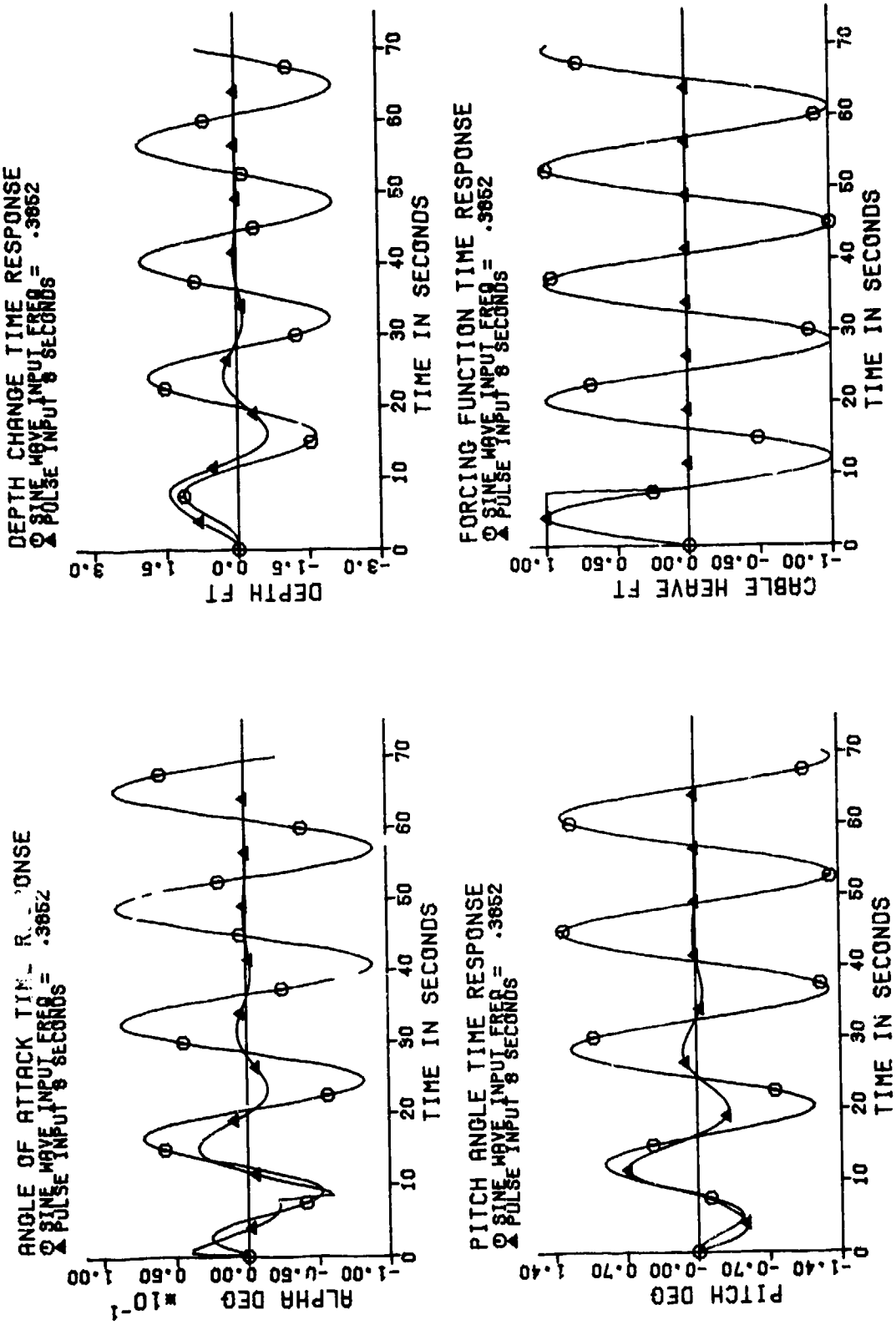

FIGURE 13. LONGITUDINAL SENSOR VEHICLE TIME HISTORIES IN RESPONSE TO A PURE HEAVE SINUSOID AND PULSE MOTION

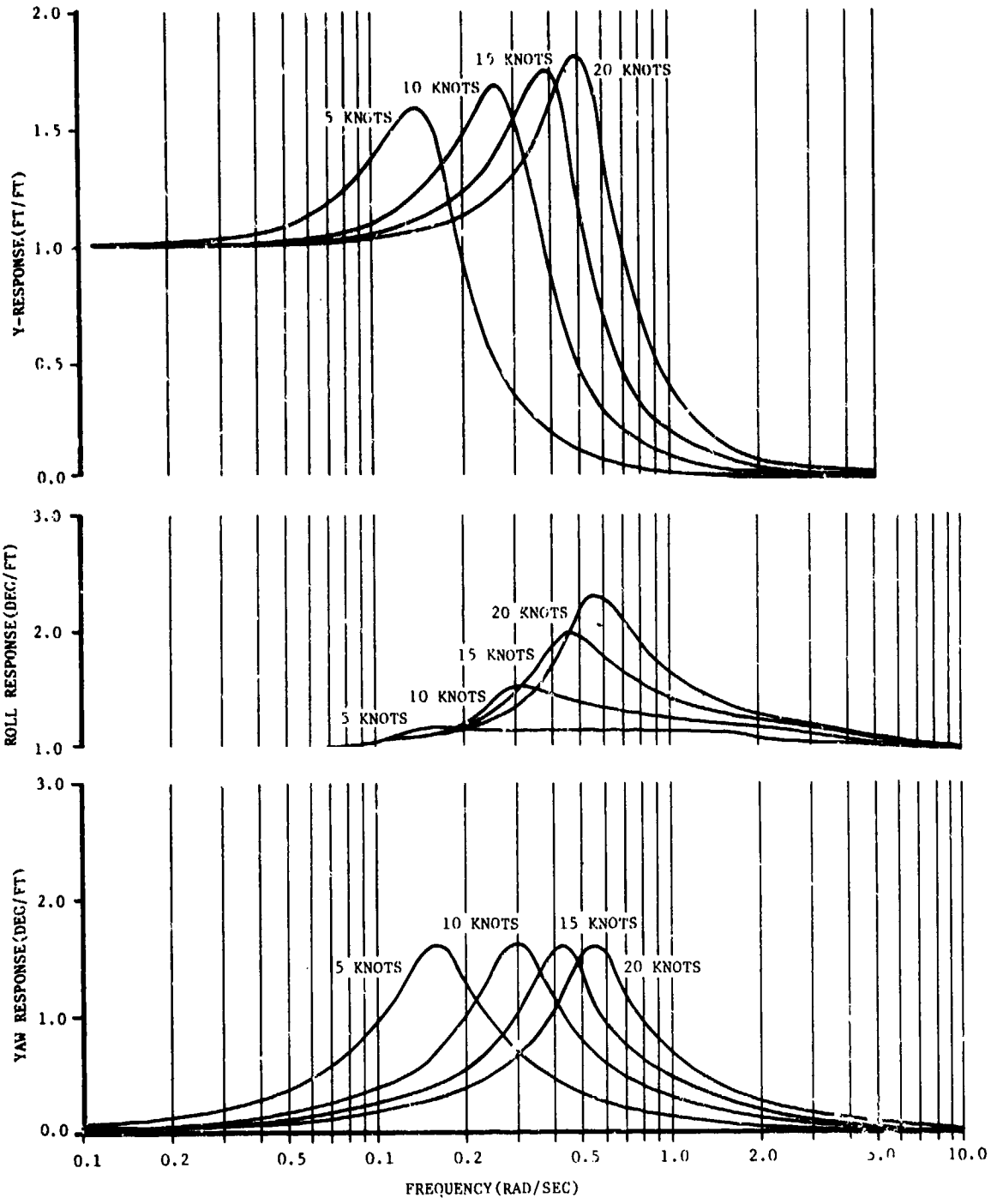

FIGURE 14. OFF-TRACK, ROLL, AND YAW RESPONSES OF SENSOR VEHICLE TO A SWAYING TOW POINT AT VARIOUS TOW SPEEDS

A review of the design requirements section will indicate that each of the motion criteria prescribed for the towed body have been met. Even in the high speed case, performance is expected to be within acceptable values unless unknown problems arise from dynamic cable motions. The motion measurement package on the sensor vehicle will signal that a problem exists should one be encountered, but in the absence of any forcing function data, the cause of the problem may remain unanswered without further tests involving additional instrumentation to measure, for example, forcing function data at the ship, the depressor, and the cable attachment point.

Before leaving the subject of vehicle response it should be noted that the effects of internal flow were not considered in this analysis. The sensor package internal to the vehicle requires a continuous flow of water from the vehicle nose to the flow outlets. In order to limit the scope of this analysis, the nose shape was considered to be hemispherical and the fluid exiting the flow outlets was assumed to have a negligible effect on vehicle dynamics.

SYSTEM TOW PERFORMANCE

CABLE SELECTION

The proper design of a towed system must include an optimization analysis on system downforce, cable scope, and winch tension at the design speed and depth. A cable must be chosen which has both the required conductor for electrical data up and down the cable and sufficient strength members which will overcome the hydrodynamic drag and depressor force. For the environmental sensing system, three existing conductor cables were analyzed to determine the hydrodynamic characteristics required to achieve a sensor depth of 500 feet at a tow speed of 20 knots. A static three-dimensional cable program[5] was used to predict the cable scope and winch tension versus downforce, as presented in Figure 15. The speed and depth requirements dictated the use of a faired cable to minimize winch tension. The winch tension curves point out that an optimum downforce exists which will minimize winch tension while limiting cable scope to a reasonable value. The dotted portions of the curves represent tension in excess of 30 percent of the cable breaking strength. Since the system is scheduled to be tested on a high speed research vessel with limited space and weight constraints for the winch, cable drum, etc., the smaller cable was highly desirable; however, the breaking strength of the cable needed to be increased. The cable diameter, therefore, was increased slightly to achieve a breaking strength of 38,000 pounds. This increased diameter in turn increased the required fairing thickness from 0.94 to 1.06 inches.

DEPRESSOR SELECTION

As noted in the previous section, the downforce required to achieve minimum winch tension was 5,000 pounds at a speed of 20 knots. This downforce can be achieved either by a weighted depressor or a dynamic lift depressor. A weighted depressor has the advantage of providing a constant downforce over the entire speed range, but could impose severe handling requirements during launch and recovery. A passive, dynamic depressor, on the other hand, has a minimal air weight but can generate large amounts of downforce proportional to the square of the tow speed. At first the variation of downforce with speed appears to be a disadvantage. However, since the cable drag also varies with speed squared, a free flooding dynamic depressor will tend to maintain depth for a

---

[5] Naval Ship Research and Development Center Report No. 4384, "A Fortran IV Program for the Three-Dimensional Steady State Configuration of Extension Flexible Cable Systems," H.T. Wang, September, 1974.

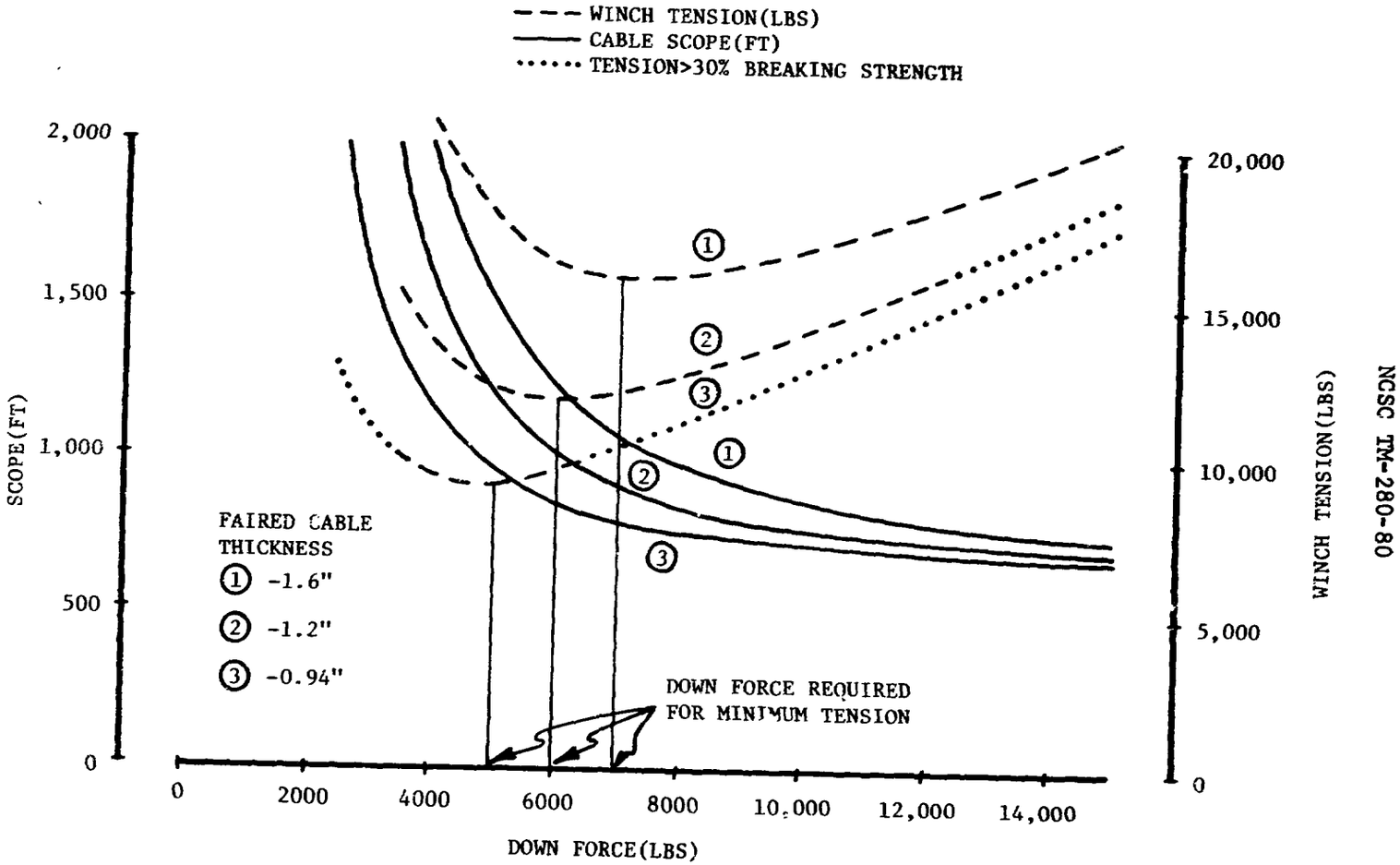

FIGURE 15. TOW CABLE PERFORMANCE FOR A DEPTH OF 500 FEET AT A SPEED OF 20 KNOTS

given cable scope as speed is varied; for a system in which depth keeping is important this becomes an advantage. Considering the advantages, it was decided that a dynamic depressor would be utilized.

Free flooding dynamic depressors have been utilized successfully for oceanographic and marine operations since 1960[6] for several system configurations. The depressor described in Figure 16 was selected for use with the sensor system. This 6-foot depressor has been tow tested up to a speed of 12 knots (a smaller depressor of the same shape has been tested up to 22 knots). The longitudinal trim tabs are interchangable to permit selection of the desired downforce at a specific speed. At speeds greater than 3 knots, the depressor will have a total drag no greater than 1/5 the downforce being produced.

In order to determine its dynamic characteristics, the depressor was analyzed[7] using the same analytical tools exercised to predict sensor vehicle performance. Since the depressor is basically a delta wing with dihedral, the analysis was not completely successful due to radical geometry of the depressor compared to conventional towed vehicle shapes*. The analysis revealed that although a stable configuration was achieved, the stability was extremely sensitive to tow point, center of gravity, and center of buoyancy position. Although further analysis is needed to completely characterize the depressor's dynamic performance as a function of speed and trim tab position, it is reasonable to assume that the steady tow performance obtained in the low to moderate speed range should also be achieved at the higher system speeds.

The desired depressor downforce at 20 knots is 5,000 pounds. The downforce in pounds at any other speed V can be determined from the relation: Downforce = $(V/20)^2$ (5,000-250) + 250. This relation was used to calculate the downforce at each speed in the speed and depth performance section.

---

6 Offshore Technology Conference Paper No. OTC 2575, "Towed Underwater Vehicle Applications from 1960 through 1975," E.C. Brainard II, May 1976.

7 Naval Coastal Systems Center Technical Note in preparation "Hydrodynamic Analysis of a Six-Foot V-Fin Depressor," C.M. Huff.

* The semi-empirical design tools for analyzing performance and stability of underwater vehicles have been developed for a general class of geometric shapes (vehicles which are predominantly near bodies of revolution with fins). Although NCSC does have techniques for analyzing zero-data base vehicles, due to their complexity their use is beyond the scope of this analysis.

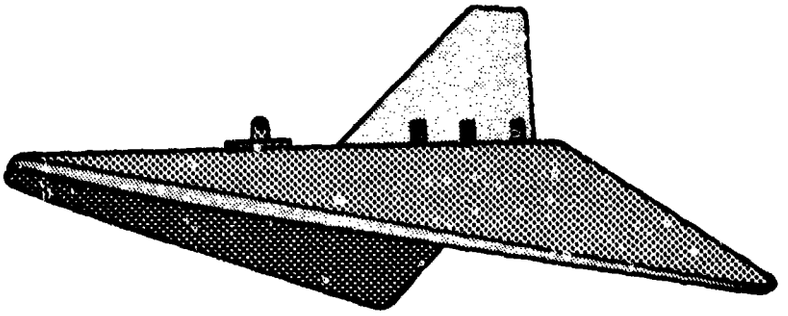

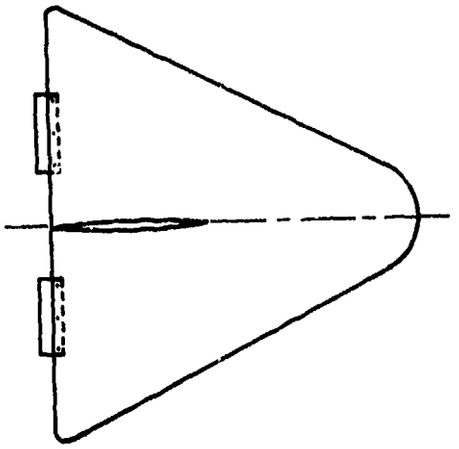

AIR WEIGHT-430 POUNDS
WATER WEIGHT-250 POUNDS
LIFT/DOWNFORCE RATIO>5:1
CONSTRUCTION-REINFORCED FIBERGLASS WITH POLYESTER RESIN

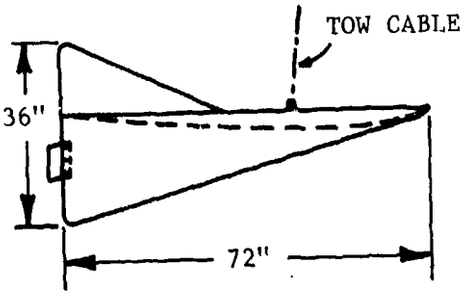

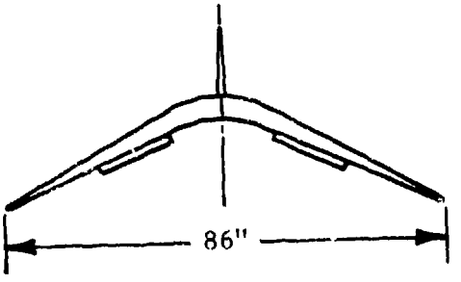

FIGURE 16. DEPRESSOR FOR THE ENVIRONMENTAL SENSOR SYSTEM

SYSTEM DRAG

The hydrodynamic resistance or drag force encountered when towing a system through the water is determined by estimating the drag of each component and then summing the results. The drag force is a function of the square of the tow velocity and is often written in coefficient form as $C_D = Drag/(\frac{1}{2}\rho V^2 S)$ where ρ = density of fluid, and S is a reference area. The components of interest in drag prediction are the depressor, sensor vehicle, cable break-out, and main cable. The depressor drag was assumed to be 1/5 of the downforce generated as noted in the previous section. The sensor vehicle drag coefficient was calculated during the hydrodynamic coefficient prediction process as C_D = 0.106, where S is the body cross sectional area of 1.77 square feet. In the case of the cable break-out (Figure 1) whose dimensions are approximately 24 inches high by 4 inches wide by 1.25 - 2.5 inches thick, the drag coefficient was estimated[8] to be 0.1196 based on body cross-sectional area. The drag area (C_D times the reference area) of the break-out/vehicle combination required by the three-dimensional cable program was specified as 0.44; this corresponds to a 10 percent increase over the predicted value to account for body and break-out protuberances.

The specification of the cable drag was more complex than any other component because the drag coefficient for the cable varies with velocity or Reynolds Number (VL/ν where L is a characteristic length in the direction of flow, and ν is the kinematic viscosity of the fluid). In order to reduce the drag, the main cable was faired with a 4.25 inch chord, 1.06 inch thick fairing section. Drag coefficients for faired cables are often approximated by selecting from Hoerner[8] the drag coefficient for an airfoil with the same thickness to chord ratio. However, as noted by Wingham and Keshavan[9], the drag coefficient of the standard fairing (Figure 1) can be three times that of an airfoil with the same thickness-to-chord ratio. It was also noted that the drag of the completed cable system is greater than the fairing drag by approximately 30 percent due to fairing gaps, fairing stops, and sawtooth misalignment. In order to ensure a conservative estimate for the cable drag for the purpose of this study, these corrective factors were utilized in the cable drag prediction. For the lower tow speeds, the Reynolds Number was often in the laminar-to-turbulent transition range, and the predicted drag coefficient ranged from 0.3 at 5 knots to 0.15 at 20 knots. These cable drag coefficients were used with the other component drags to predict the cable speed and depth performance data presented in the next section.

---

[8] Hoerner, S.F., Fluid Dynamic Drag, Published by Author, 1965.

[9] Ocean Engineering, "Predicting The Equilibrium Depth of a Body Towed by a Faired Cable," P.J. Wingham and N.R. Keshavan, volume 5, pp. 15-35, Pergamon Press, 1978.

Due to the high test speeds at which the system will be towed, trailing edge extensions were added to the fairing trailing edge to help ensure that the fairing section did not kite. The extenders move the center of pressure of the fairing well aft of the center of rotation[10] to ensure that any lift generated by the fairing will also create a moment to return the fairing to zero angle of attack. The extenders themselves affect the total fairing drag only slightly.

DEPTH AND SPEED PERFORMANCE

Utilizing the drag data presented in the previous section, cable catenaries were predicted for different system configurations as functions of tow speed and depth achieved. The static three-dimensional cable program developed by Wang[5] was used to predict the steady state cable performance data. In the data generated, it was assumed that the sensor vehicle break-out was separated from the depressor by 106 feet of cable which yields a depth difference of 100 feet. Also, downforces of 5,000, 2,922, 1,438, and 547 pounds were used at the corresponding velocities of 20, 15, 10, and 5 knots.

The cable catenaries for placing a single sensor vehicle at a depth of 500 feet (depressor depth of 600 feet) is presented in Figure 17 for speeds of 5, 10, 15, and 20 knots. An interesting and valuable property of this type of plot is that it defines cable shape for depressor depths of less than 600 feet as well. For example, the cable catenary for the depressor at 400 feet is that portion of the catenary from the 600 feet depth to the 200 feet depth; similarly a 200-foot depressor depth is described by the shape from 400 feet to 600 feet. This property of the cable catenaries was used to generate the cable performance chart presented in Table 9. These same data are displayed graphically in the cable performance diagram of Figure 18. Given a cable scope, the curves can be used to predict vehicle or depressor depth, trailback, and steady state winch tension; for example, for a 5-knot tow with 500 feet of cable deployed, the depressor and sensor are located at depths of 400 and 300 feet, with trailbacks of 240 and 235 feet, respectively, while the steady state winch tension is 1,100 pounds. It should also be noted that those data can be used to determine cable scope required to reach any desired depth, and interpolation may be used to approximate data for speeds other than those presented.

The effects of towing multiple sensor vehicles can be evaluated by examining Figures 19 and 20. Figure 19 compares the catenaries for one,

---

10 Ocean Engineering, "Some Towing Problems with Faired Cables," J.F. Henderson, volume 5, pp. 105-125, Pergamon Press, 1978.

5 NSRDC Report No. 4384, *op. cit.*

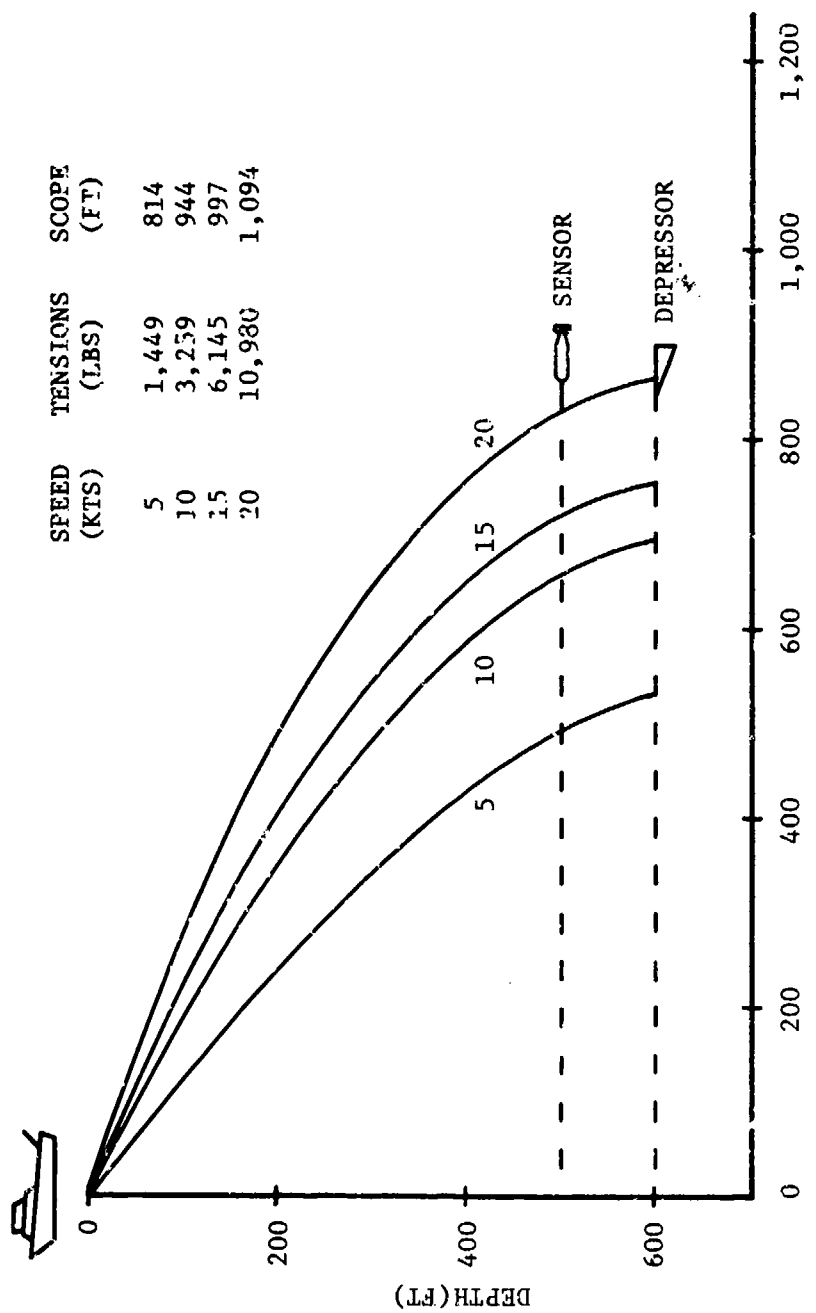

FIGURE 17. CABLE CATENARIES FOR A SINGLE SENSOR VEHICLE AT SPEEDS OF 5, 10, 15 AND 20 KNOTS

TABLE 9

CABLE PERFORMANCE DATA FOR SINGLE SENSOR VEHICLE TOW

SCOPE (FT)	SPEED (KT)	DEPRESSOR DEPTH (FT)	DEPRESSOR TRAILBACK (FT)	SENSOR DEPTH (FT)	SENSOR TRAIL-BACK(+PIGTAIL) (FT)	WINCH TENSION (LBS)
200	5	179.23	84.93	79.23	80.12	779.46
	10	176.76	88.67	76.76	83.60	1835.13
	15	176.86	88.26	76.86	83.88	3571.82
	20	175.45	90.51	75.45	85.31	6064.53
300	5	257.34	147.32	157.34	142.51	889.20
	10	250.43	156.20	150.43	151.13	2019.36
	15	250.02	156.34	150.02	151.96	3868.87
	20	246.66	160.63	146.66	155.43	6558.09
400	5	330.37	215.60	230.37	210.79	999.08
	10	316.98	230.80	216.98	225.73	2209.17
	15	315.39	231.96	215.39	227.58	4181.89
	20	309.40	238.44	209.40	233.24	7084.09
500	5	399.53	287.82	299.53	283.01	1108.56
	10	377.72	310.22	277.72	305.15	2401.56
	15	374.20	312.81	274.20	308.43	4503.93
	20	365.03	321.50	265.03	316.30	7628.88
600	5	465.67	362.81	365.67	358.90	1217.49
	10	433.70	393.06	333.70	387.99	2594.98
	15	427.52	397.40	327.52	393.02	4831.02
	20	414.70	408.27	314.70	403.07	8184.54
700	5	529.43	439.85	429.43	435.04	1325.84
	10	485.78	478.43	385.78	473.36	2788.61
	15	476.21	484.72	376.21	480.34	5160.80
	20	459.37	497.73	359.37	492.53	8746.36
800	5	591.27	518.43	491.27	513.62	1433.64
	10	534.59	565.70	465.70	529.52	2982.02
	15	521.00	574.13	421.00	569.75	5491.87
	20	499.84	589.17	399.84	583.97	9311.45
814	5	600.00	529.80	500.00	524.80	1449.05
900	10	580.67	654.44	480.67	649.37	3174.98
	15	562.46	665.12	462.46	660.74	5823.37
	20	536.72	682.12	436.72	676.92	9878.05
-	5	-	-	-	-	-
944	10	600.00	692.48	500.00	688.48	3258.87
997	15	600.00	754.71	500.00	749.71	6145.29
1000	20	570.54	776.22	470.54	771.02	10445.05
-	5	-	-	-	-	-
-	10	-	-	-	-	-
-	15	-	-	-	-	-
1094.31	20	600.00	865.80	500.00	390.60	10979.50

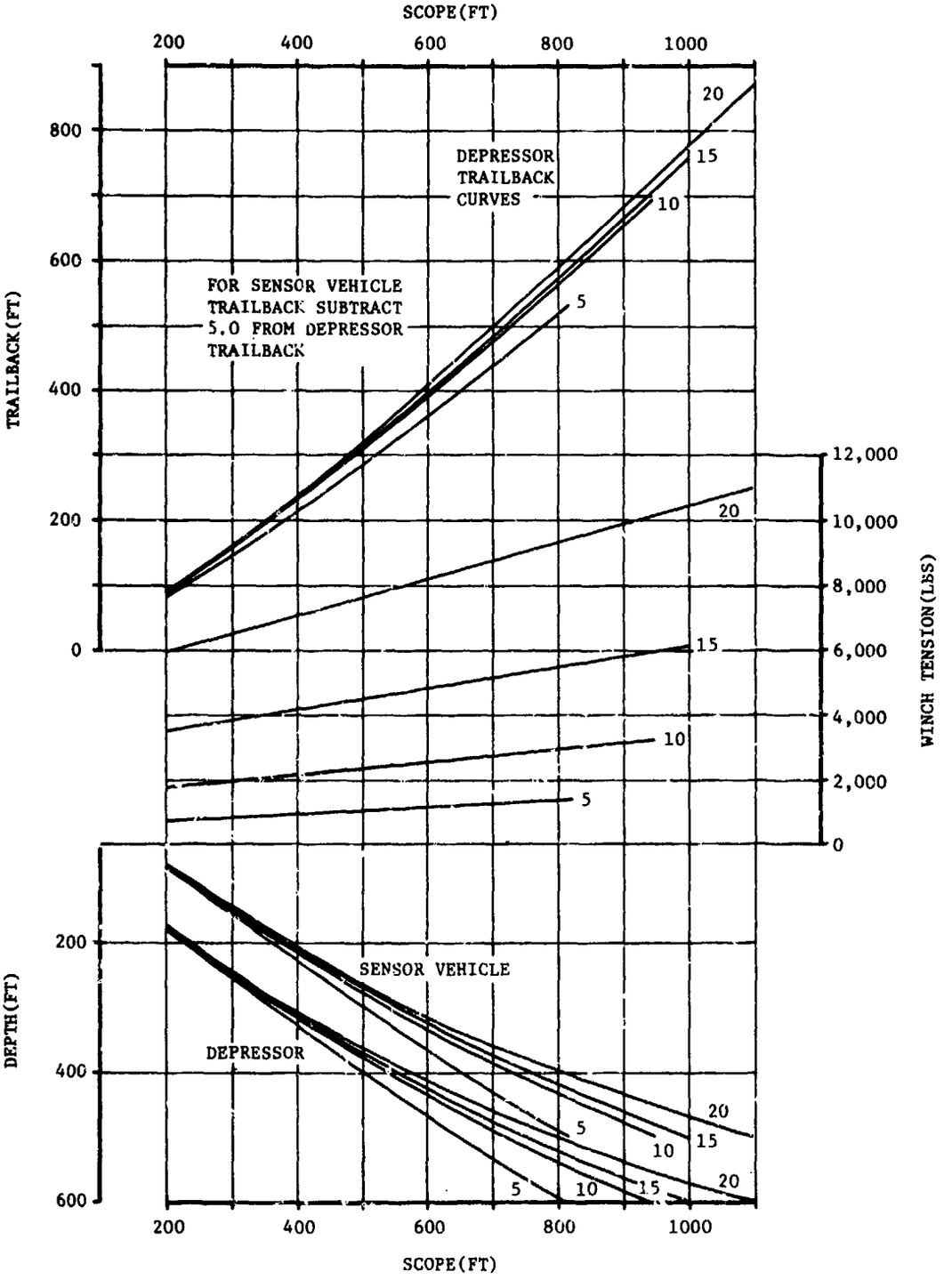

FIGURE 18. CABLE PERFORMANCE DIAGRAM FOR SINGLE SENSOR VEHICLE TOW

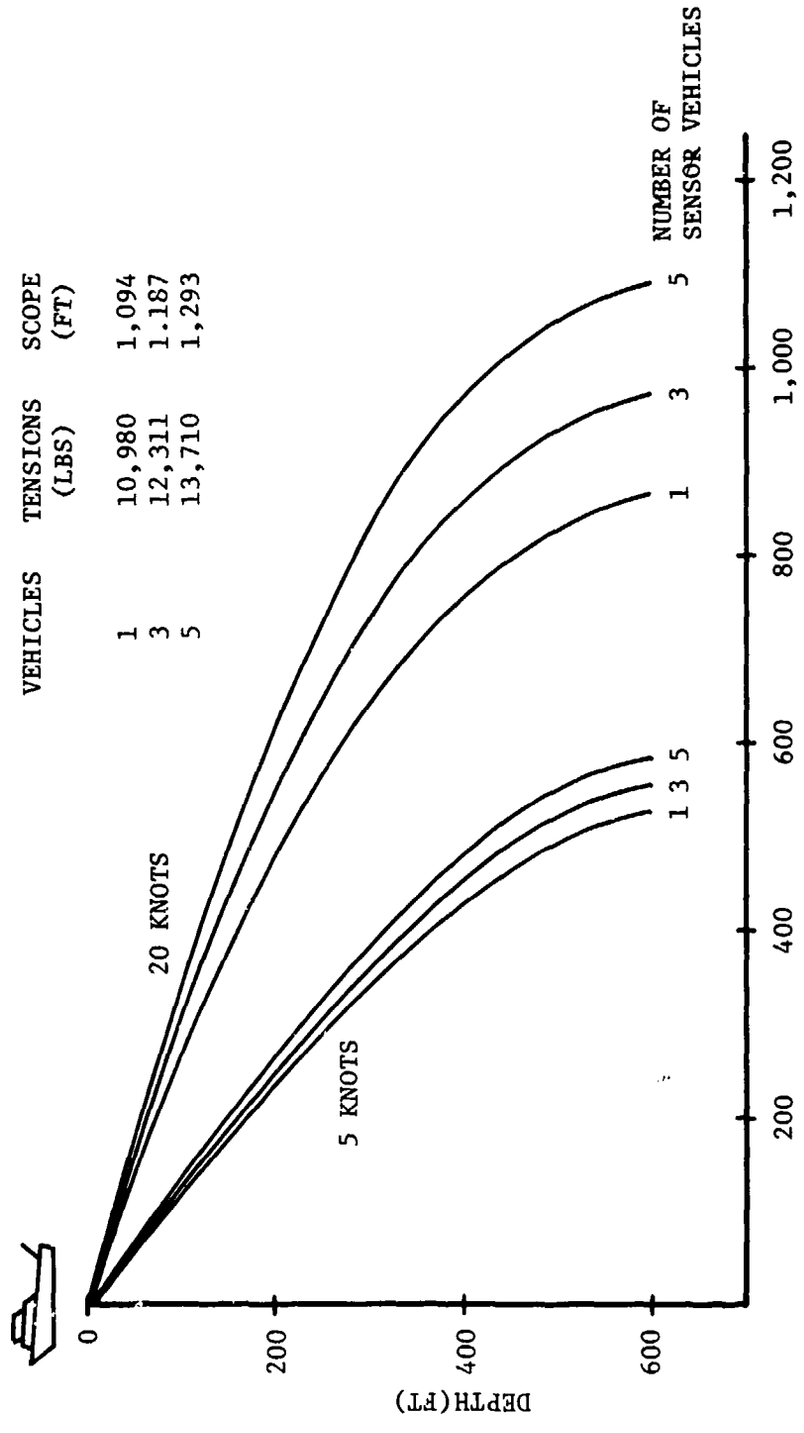

FIGURE 19. CABLE CATENARY COMPARISON FOR MULTIPLE SENSOR VEHICLES AT SPEEDS OF 5 AND 20 KNOTS

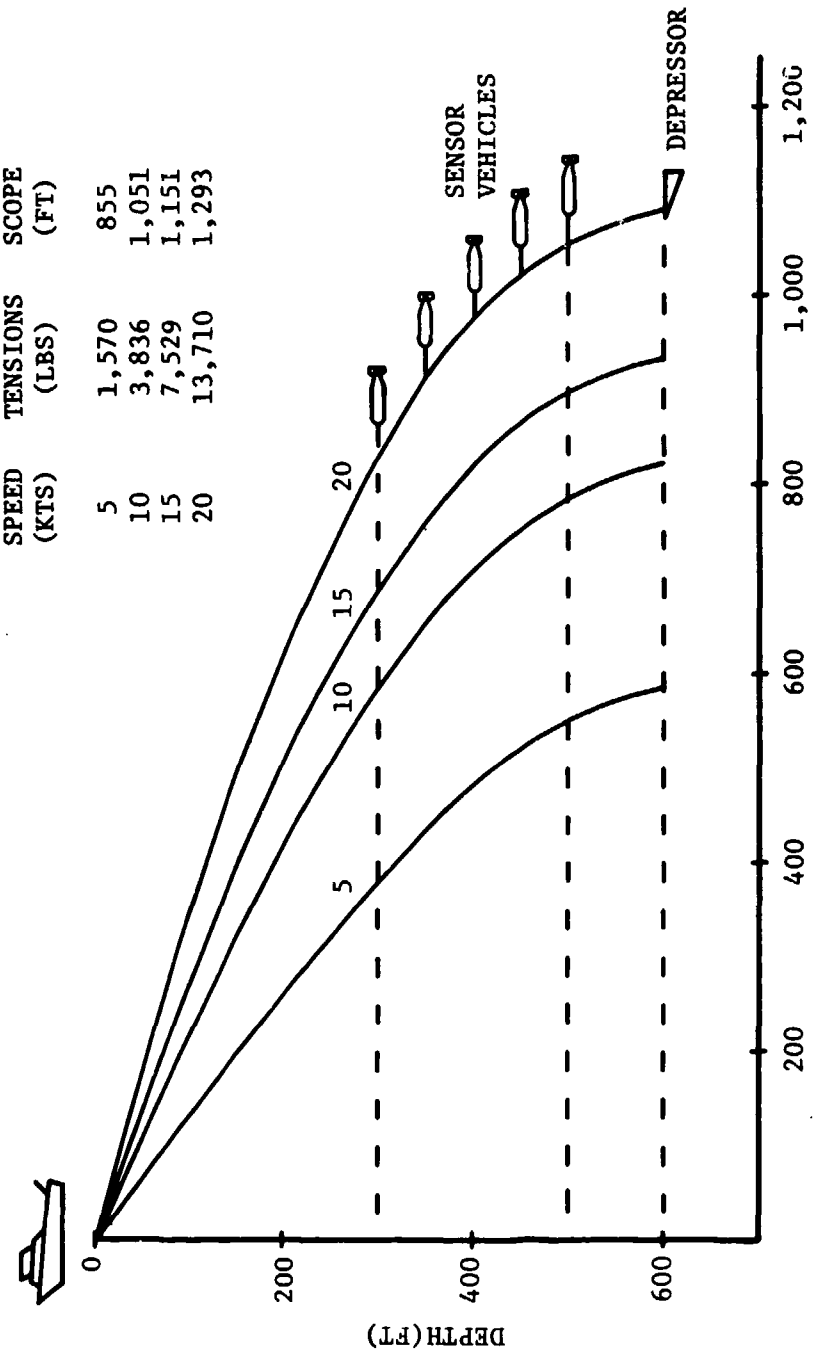

FIGURE 20. CABLE CATENARIES FOR FIVE SENSOR VEHICLES AT SPEEDS OF 5, 10, 15 AND 20 KNOTS

three, and five sensor vehicles at speeds of 5 and 20 knots, and also presents their respective scopes and winch tensions. In the case of the three-vehicle tow, the vehicles were located at approximate depths of 500, 400, and 300 feet, while for the five-vehicle tow the depths were 500, 450, 400, 350, and 300 feet. The data indicate that in going from one sensor to five while maintaining a 600 feet depressor depth at 20 knots, the scope increases 200 feet (approximately 50 feet per extra vehicle). Figure 20 presents data at all four speeds for the five-vehicle tow.

Before concluding the cable performance section, three important points concerning tow performance must be considered. The first is that the cable analysis is a static, steady state tow analysis; thus, the effects of any time-dependent or frequency-dependent cable motions have not been considered. Even though the system is essentially cable-dominated, the development and utilization of a robust dynamic cable model was beyond the scope of this task. Dynamic effects have been neglected successfuly for many low speed, moderate depth (low downforce) systems; however, as speed and depth increase, neglecting dynamic effects becomes more questionable. Second, the cable performance is a very strong function of the depressor downforce; thus, if the downforce delivered is significantly different from the design value, then the cable performance data will be qualitatively correct but quantitatively in error. Also, since the sensor vehicle has no active control system, the mean depth will be a direct function of the depressor depth. The third and final consideration is that of ship speed. The tow performance data generated above assume that the ship speed is constant; any variation will, in effect, produce a new steady state cable catenary modifing the depressor and sensor equilibrium depth as noted in Table 10. Thus, depending on how accurately the ship can maintain constant speed, overall depth-keeping performance may be affected by speed variations.

TABLE 10

EFFECTS OF TOW SHIP SPEED VARIATION ON DEPTH KEEPING

Low Speed Variation Scope = 814 feet	Speed (kts)	5.5	5.0	4.5
	Depth (ft)	593	600	606
High Speed Variation Scope = 1094 feet	Speed (kts)	21	20	19
	Depth (ft)	596	600	605